UNIVERSITY OF TWENTE.

Dept Health Technology Implementation

Implementation of 3D technologies for quantification and improvement of clinical diagnostics

Sandipa Sharma

Master Thesis Biomedical Engineering

November 2020

Examination Committee

Prof. Dr. Ir. R.M. Verdaasdonk

Dr. Ir. N. Bosschaart

Dr. V. Groenhuis

Biomedical Photonics Imaging Group

Faculty of Science & Technology

University of Twente

P.O. Box 217

7500AE Enschede

Netherlands

Summary

The following work is a cumulation of my master thesis for the Biomedical Engineering Photonic Imaging Group at University of Twente within the Faculty of Science & Technology. This thesis will explore the necessities for incorporating a 3D scanning system into the workflow for particular clinical applications.

With the known limitations of 2D medical imaging systems currently used in clinics, the increase in development and availability of 3D scanners and images can address these shortcomings. Current 2D photography systems include MRIs, X-rays, CTs, and ultrasounds, which provide information about the internal mechanisms of the human body. However, none of these devices are able to provide quantitative images of the complex surface of the human body. This is important for monitoring the development of bodily changes, measuring surface area of skin ailments, and planning or demonstrating surgical techniques.

The first experimental aspect of this research is to examine the ability of the iPhone X to make a 3D scan, since this is a novel device which has yet to be used in the clinical setting, but has shown the potential in being more accurate. The second focus of this study will be to determine the main steps needed to successfully process a 3D scan for quantitative measurements. The goal is that the steps can be applied seamlessly to any necessary application while maintaining accuracy. This paper will primarily target the application of 3D scanning the breast and obtaining volume measurements. This particular application is helpful in monitoring breast development for transgender studies and breast reconstruction. Breast phantom scans were shared for this study from the Department of Internal Medicine at the Amsterdam UMC.

In this project, 3D scans were obtained using the iPhone XR, and a workflow was defined for processing the scan that can be used to gather accurate volume measurements for future clinical applications. While the general steps have been detailed, achieving accuracy depends on the shape complexity of the object and the experience of the operator.

Acknowledgments

Dear reader,

My long, life-changing journey is coming to an end. In 2017, I quit my comfortable job and left behind my treasured Chevy Volt and beloved circle of family and friends, packed my dog, and traveled to a different country where I did not know anyone, let alone the language, to study for a Master's degree at the University of Twente. I have been away from academia for so long, my undergraduate knowledge was rusty, and the grading system in the Netherlands was very different than what I was used to in America. What was supposed to be 1 year of coursework, ended up being 2 years due to the difficulty of the courses. I was grateful to have my health, until 1.5 years into my coursework, after I had only a few more classes to finalize, I broke my ankle and had to get surgery to fix it. In a country where biking is our lifeline, I was instructed to not walk for 2 months. Even after I could walk, I had a long road to recovery ahead of me. I have to deal with this, alone in a foreign country, while doing a difficult study. I missed my car immensely.

Fast forward to now, 2020! One more course to be completed, and my internship at DOVIDEQ Medical had given me a taste for the industrial work I hope to achieve after my study. Beginning of this year I joined the Biomedical Photonic Imaging Group to start my thesis under the guidance of Prof. Ruud Verdaasdonk. While things were starting to feel normal again, with the final stretch of my study within sight and being on the familiar campus, the unfortunate COVID-19 hit. Thanks to the Dutch government and the University of Twente leadership for taking precautions seriously, I was never infected and able to continue my thesis safely from home. This slowed things down, and provided less facetime with helpful people and equipment, however for the most part I was able to continue onwards. I want to give my most sincere gratitude to Ruud for making himself available when I had doubts, checking in with me, and giving me a pep talk when I am overwhelmed with the details. In midst of a pandemic and developing alternative ventilation masks for a very real problem happening around the world, he provided a lot of insightful feedback and helped me reach my goal of getting a Master's degree.

I also would like to thank some people from the Amsterdam UMC group and MST Enschede. Thank you to Benthe Dijkman, Christel de Blok, Professor Martin den Heijer for providing the scans from the various 3D scanners. Also thank you to GOM Inspect master Niels Liberton for helping me with some of the GOM Inspect issues I encountered. Finally thanks to Thomas van Kuipers, another student who did his internship at MST Enschede on a relating topic, for discussing information and results with me.

On a more personal level, I want to thank my family and friends individually. First of all, to the amazing European friends I made while studying abroad. Muchas gracias and veel dank to my fellow war veterans Javier and Diana for enduring my ranting and suffering through the classes with me. Also grazie molto to Giacomo for being the perfect Italian nonna I wish I had and cooking delicious Italian food, even when I couldn't walk. I definitely would not have survived classes without you guys!

To my friends back home: Kit, Sam, Grace, Sunny, Allison – thank you for somehow managing to be there for me while being across that pond we call the Atlantic. Your phone calls, video calls, sharing memes, continued to give me the comfort home and feeling understood in a country where I feel constantly misunderstood. And helped me refresh my English which seems to be deteriorating!

Thank you to my families, and I say family plural because I am lucky to have one in America and now in the Netherlands, the Sharma and Vlot fam. I definitely could not do this without the support of my mom and dad back home. Financially, they kept me afloat, but also making sure I have a place to come back to after all is said and done. Meanwhile my Dutch family provided some wonderful memories of my time here in the Netherlands, so that it was not solely about my study, and kept me well-fed and sane.

My final thanks goes to my amazing boyfriend, lieverd, love of my life, Maurice. He took me to the hospital when my terrible accident happened, cooked for me, and kept me company when I was stuck at home. Also he provided a safe and comfortable place for me and my dog to live when I couldn't find any pet friendly space. Thank you for making sure the only thing I had to focus on was my recovery and my study, and for being such a helpful soundboard throughout my study. I couldn't ask for a better partner/roommate/boyfriend and I know for sure I would not have made to this point if it weren't for him.

Thank you to everyone for making this project possible and helping me "achieve mastery".

Table of Contents

1. Introduction

1.1 Context of problem

Patient measurements, such as body size and shape, are good indicators to assess health status and determine treatment. Clinicians traditionally perform manual measurements to diagnose diseases and determine treatments. With developing technology in medical imaging, such as computed tomography (CT) scanners, X-rays, magnetic resonance imaging (MRI), and ultrasound, it is possible to get 3D internal images of a patient. These images are so regularly used in clinics, that medical imaging is considered the gold standard for comparison to novel techniques. For 3D surface measurements, 3D surface scanners that are available and being used in industry, have shown to be low cost, efficient, noninvasive, and user-friendly, therefore appealing for clinical applications [10]. Within a few seconds, these scanners non-invasively provide a patient's body shape, size, texture, and color, further improving the gold standard of medical photography. Additionally, since this technology automatically extracts measurements during scanning to create a 3D model, this eliminates any measurement errors due to human transcription. Medical professionals are able to use these external measurements to assess nutritional status, developmental normalities, to calculate drug dosages, and to produce fitted prostheses [10].

Apart from providing an image with surface depth information, 3D scanning technology can further improve medical photography in various ways. Detailed information about body size and shape could replace the current reliance on body mass index (BMI), which is used to quantify traits but is not an accurate marker for diseases, since people with different BMIs are not always the same shape [11]. A study conducted by Daniell et al concluded that different body shapes within BMI categories can be characterized using volumes, which were obtained from 3D scans [11]. Therefore, the ability to obtain accurate and noninvasive volume quantifications is required for treatment and diagnostics. Another benefit is that 3D scanning is ideal for daily use because the resulting information is reproducible. The simplicity of operating the 3D scanner and ease of obtaining and sending data online allows for repeatable results [12]. Another study tested required new users and skilled users to perform anthropometric scans using a 3D photonic scanner [13]. With a limited amount of training, the new operators were able to perform at an acceptable level comparable to the skilled operator. This further illustrates the reliability of the measurements, despite the variation of experience from the different operators. Having easy access to technology that can be used daily can assist in monitoring treatments and assessing the effects of the treatment. Much like current medical imaging devices, such as X-rays, CT scanners, MRI, and ultrasound, 3D scanners contribute to the ability to check the human body through a simple surface scan. In contrast to those current accepted medical imaging devices, it provides quantified surface information.

Recent advancements in 3D scanners have proven its capabilities in the medical field. This consists of human body metrics that provide highly accurate digital maps of the body used for developing measurements or visualization, creating images of the skin surface area for precise measurements without the need for replicas, and providing 3D visualization for doctor-patient interaction in cosmetic surgery or assessing risk for planned surgeries [12]. The general process for creating a medical model using a 3D scanner is as follows and is illustrated in Figure 1:

1. **Developing the physical model that will be scanned.** For example, this would be the breast of the patient or a phantom breast model.
2. **Scanning the model using a system that can convert the model to standard triangle language (STL) format.** Different systems can be used to scan the patient for varying results. While it is of utmost importance to obtain measurements that are accurate and provide the highest resolution, when scanning a human patient, the comfort and practicality of the system should be taken into

consideration. This consideration of comfort is different compared to scanning a standalone phantom, which is an object that can be placed in any position.

3. **Generating the model on the computer for segmentation or modification.** The original file will contain some noise that will need to be removed. Additionally, segmenting the relevant part of the mesh will help process and analyze the 3D model.
4. **Inspecting, testing, or analyzing the 3D mesh for medical use.**

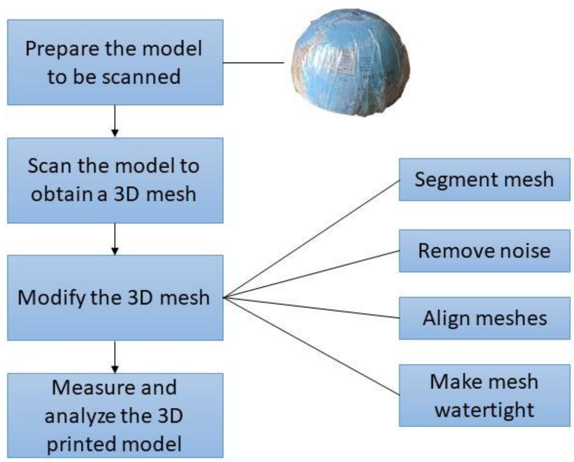

Figure 1: Flow chart process illustrating from original model to final 3D printed model for measurements

Current 3D scanners have been introduced into the clinical field, and are able to scan the exterior of the patient and provide some metrics. The prices of these scanners can range from €500 to €30000. However new smart phones, such as the iPhone X, contain facial recognition functions, and therefore are capable to serve as a scanning device if paired with an appropriate application. The iPhone X is more affordable and accessible, therefore the focus of this study is to explore the potential in utilizing this functionality for future medical applications.

1.2 Problem definition

While 3D scans produce visually appealing models, it is most helpful in a clinical setting if it contains quantitative information. These measurements are especially helpful for transgender hormonal therapy studies, breast reconstruction, and in monitoring lactation in new mothers. Therefore, the application focus will be on measuring breast volume. However, there are some challenges in systematically observe the 3D shape of the breast. Various landmark examples are shown in Figure 2. One study measured nipple to medial border (MR), nipple to lateral border (LR), and nipple to inframammary fold (IR) to calculate breast volume using a formula [6]. Whereas in another study the chosen landmarks were taken from the sternal notch (SN), nipple (N), inframammary fold apex (IMFA), umbilicus (UMB); these measurements were based on the vector lengths of these points [7]. In the third example shown in Figure 2, similar landmarks are used in addition to the points along the upper and lower inframammary folds to identify the curvature of the thorax when segmenting the breast from the torso [9]. As the examples show, it is important to take the following uncertainties into consideration when measuring the breast: (1) defining the shape of the breast is ambiguous, therefore selecting anthropometrical points depends on the operator; and (2) quantifying the curved surface of the breast is complex, and mathematical equations do not provide simple parameters to adopt to each individual [8].

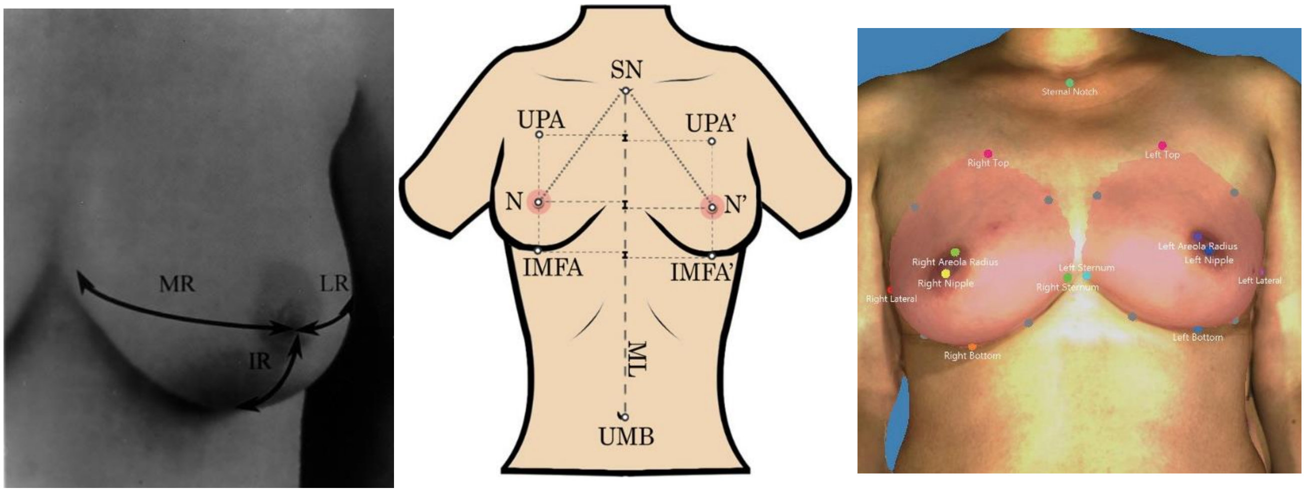

Figure 2: Landmarks and dimensions used in various breast volume measurement protocols. (Left) Dimensions MR, LR, IR on a patient breast used for calculating volume [6]; (Middle) Landmarks SN, N, IMFA, UMB [7]; (Right) Additional landmarks for upper and lower breast borders to determine thorax contour at the breast base [9]

Classical techniques to measure and monitor breast development are not quantitative, uncomfortable for the patient, and are not generally recognized methods in clinics [2]. Some methods tested in accuracy for measuring breast volume include mammography, thermoplastic molding, modern imaging procedures such as CT and MRI, Archimedes principle, and anatomical measurements with mathematical models [6]. These methods produce different results, and each has its advantages and disadvantages. Anatomical measurements equate the breast volume to a half-ellipsoid, and the measurements for the parameters of the formula are obtained directly from the patient or indirectly via 2D images [2]. Anatomical measurements were the easiest to obtain and tolerable for patients, however the mathematical formula for breast volume and shape is open to criticism [6]. The mammography method is comparable to the anatomical measurement method, since a half-ellipsoid geometry is applied to the two-dimensional image and appropriate mathematical models are used to calculate the breast volume [2]. The Archimedes method is based on the Archimedes' principle of water displacement. A calibrated cylinder is placed against the thorax wall, which measures the tissue part of the breast as the displaced breast volume. The Archimedes method was acceptable, but some patients had difficulty performing the test adequately [6]. Modern imaging techniques such as CT and MRI require the patient to be placed on their backs in a scanner, and the breast volume is computed by summing together the cross section images [2]. However, MRI is too expensive to be performed routinely. Finally, thermoplastic molding creates a three-dimensional negative cast of the breast, which can be filled with water or sand to determine breast volume. Thermoplastic molding seemed to be the best method, because it provided a 3D model, as well as a measurement [6]. Alternatively, the same can be accomplished using a 3D scanner, but is much easier, less invasive, and allows the patient to be a more natural position than in the thermocasting method. Additionally, 3D technology has the ability to quantitively evaluate symmetry, volume, shape, contour, surface, and distance measurements [2].

The most current method being used at Amsterdam UMC (location Vrije University, VU) is a function within the Vectra 3D scanner. This scanner, based on photogrammetry, identifies anatomical points of interest and uses those points to calculate the volume. These landmarks consist of the jugular notch, midclavicular lines, the nipples, the areola borders, the IMF, and the lateral and medial IMF. Although this device easily obtains breast volume measurements, it is apparent in previous studies that it results in models with the lowest resolution [14]. As new 3D technology continues to be developed and becomes readily available, there are additional options to be explored to expand on the usefulness of 3D images in clinics. Considering the convenience and ease of 3D surface scanning, it is beneficial to explore its usability for measurements of the human body.

The overall goal of this project is: (1) to test the possibilities of using the iPhone X to obtain a 3D scan; (2) to process the scan using various software to obtain accurate measurements; and (3) to quantify the resulting 3D image that closely resemble the original object that was scanned (as shown in Figure 1). An optional step, that is not covered in the scope of this research, is using the obtained 3D image to make a 3D print of the mesh. The process will be first completed using a phantom with a defined geometric shape that is simple to scan and measure. After scanning the model, the scan must be processed using various software packages. Measurements can be obtained by using some of the same software packages that were used to process the mesh. Identifying the advantages and ease of use for these software packages, along with the quality of the 3D scans obtained from the iPhone X, will help streamline a process for the application of 3D scans in a clinical setting. An optimal workflow would consist of minimal switching between software packages, should be easy for new users to learn and navigate, and utilize automatic functions for cleaning and obtaining measurements from the mesh. Figure 4 illustrates the optimal workflow of scanning the mesh to obtaining volume measurements. With a user friendly workflow, there is less processing time and quicker patient turnover. Finally, the process will be tested on some breast phantoms with known volumes to see how the scanned volumes compare.

1.3 Research question

The goal of obtaining measurements of the breasts with the iPhone X will be divided into questions:

1. **How are the boundaries of the breast defined?** Defining this will largely affect how the final volume results are obtained.
2. **What steps and software packages are needed to process the model of simple objects with known volumes?** This would ideally be achieved using a single package, however, it may be necessary to use multiple packages due to software limitations.
3. **How can this validated process in research question 2 be applied to a complex model of a breast phantom? How do these results compare?** Using the validated process from research question 2, volume measurements of the breast models, provided by Amsterdam UMC, will be collected. The volume results will be compared to the known volume.

With these questions answered, we will be able to understand how the overall clinical flow should be for the application of the iPhone X in quantitative research of body metrics.

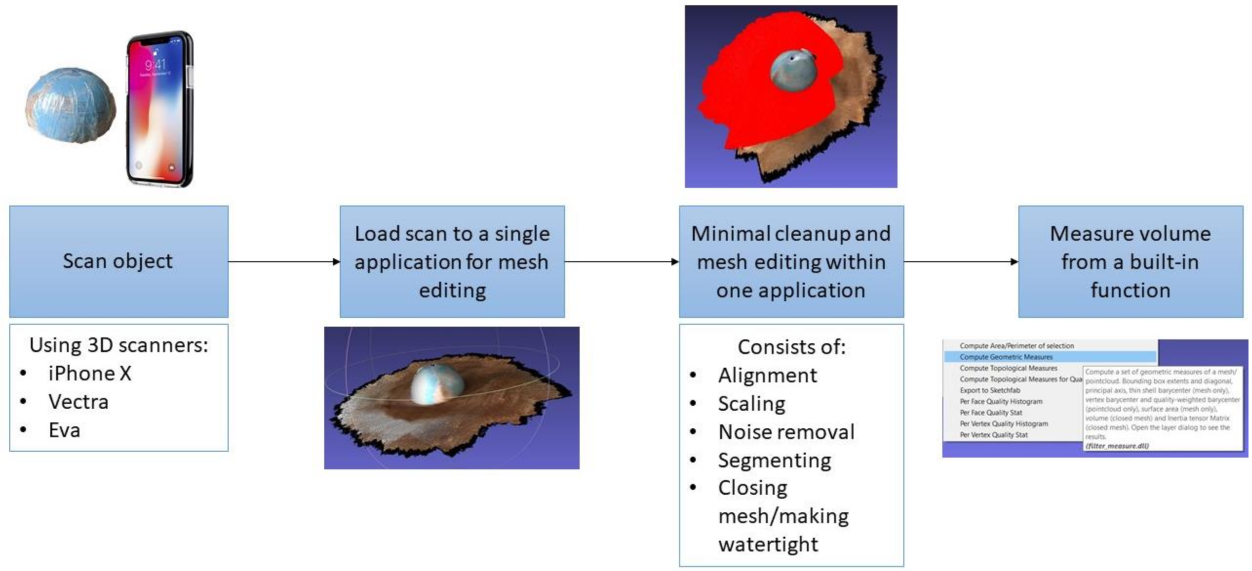

Figure 3: Optimal workflow of quantitative 3D scanning from scanning the object to acquiring measurements

1.4 Structure

The first phase would be to mathematically dissect the geometry of the breast in 3D. The structure of the breast is complex, and many landmarks are used to determine the bounds of the breast. The bounds are important for segmenting the breast from the torso, as this could influence the final results. These landmarks can be applied to the model that is scanned, and then are visible in the 3D mesh for segmentation. The determined breast bounds will be explored theoretically for future studies. However, for validation, a phantom of a half sphere will be used.

The second phase would be to segment the mesh. This would result in solely the mesh of interest, so in the case of the breast, it would be the breast without the torso attached. Additional tasks in this step would be to clean up the scan, and prepare it for quantification and 3D visualization. This is not yet streamlined, and there are various software packages that can accomplish these tasks.

The third phase would be to obtain various measurements, including volume and lengths, using software packages. These measurements will be compared to measurements from a gold standard method. For volume, the gold standard is the water displacement method. For length, this can be measured on a phantom with a tape measure.

The fourth and final phase is to determine the workflow of how this can be applied to the clinical workflow for transgender breast growth related studies and breast reconstruction surgery. Certain steps and applications are required in order to successfully obtain measurements of a 3D scan.

The flowchart Figure 5 illustrates the main phases of this research.

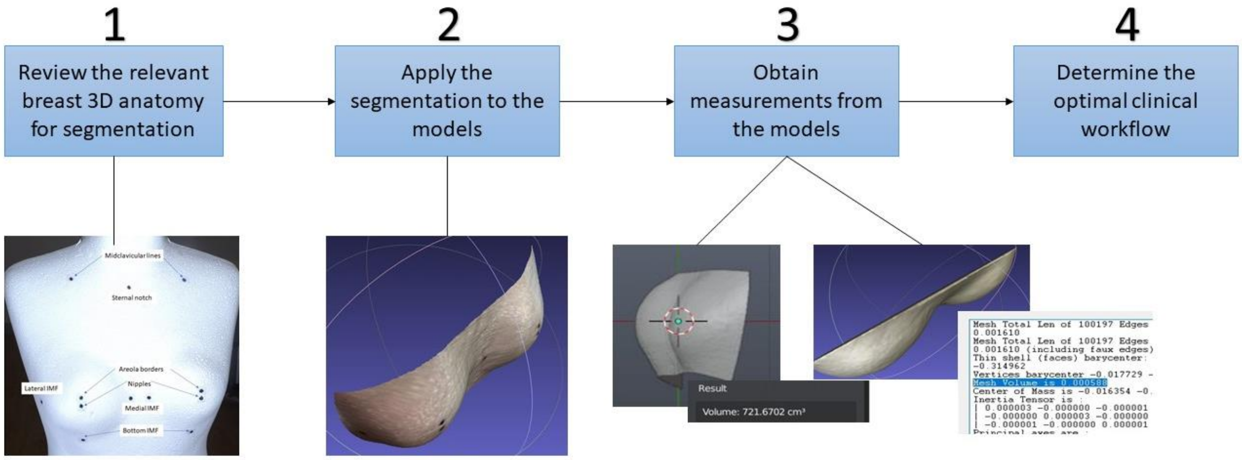

Figure 4: Flowchart representing the main phases of this research and visual examples of each section

2. Materials and Methodology

2.1 3D scanners

There are many types of 3D scanners already in existence, and for anthropometry, they are most commonly laser and light-based technologies [13]. The breakdown of the classifications of 3D scanning techniques can be seen in Figure 5, which are divided into contact and non-contact scanners. The focus of the paper will be on the non-contact technology, which can be further divided into active and passive categories. Passive techniques use the information already at the scene to build a 3D model, whereas active methods introduce controlled information, such as structured light, to overcome the limitations of passive methods. There are three main working principles of 3D scanners using photogrammetry, stereovision, and structured light [14]. Photogrammetry can be a passive or active 3D imaging technique. It involves using a single camera to take a sequence of photos of the object from different angles. By using triangulation, the 3D coordinates of the 2D points that are present in camera views are calculated. In the active photogrammetry case, the object would be projected with a structured pattern to determine the image in 3D space. Stereovision uses multiple cameras located in different positions around the object to capture the same scene in different viewpoints. Finally, structured light is an active technique in which light patterns with known spacings are projected onto the object. By moving the camera around the object or rotating the object, it is possible to capture the different angles of the object, and create a 3D reconstruction based on the deformations of the projected pattern. The advantage of this technique is the speed at which data is acquired and the accuracy level [15]. The advantage of using the stereovision and fringe projection is the speed, since they are able to scan an entire view with multiple points within seconds [16]. This also reduces any chance of distortion caused by motion, which could create issues using the photogrammetry method. However, photogrammetry can be cheaper, since it only requires a digital camera and no special hardware. The downside of this method is its reliance on the resolution of the camera and natural contrast/texture in order to get accurate results; therefore it is important to use high quality cameras [16]. The natural lighting conditions for passive photogrammetry need to be controlled to capture the object details. Despite this, there are 3D scanners available that are able to combine passive and active stereo photogrammetry to achieve higher quality 3D surface images [16].

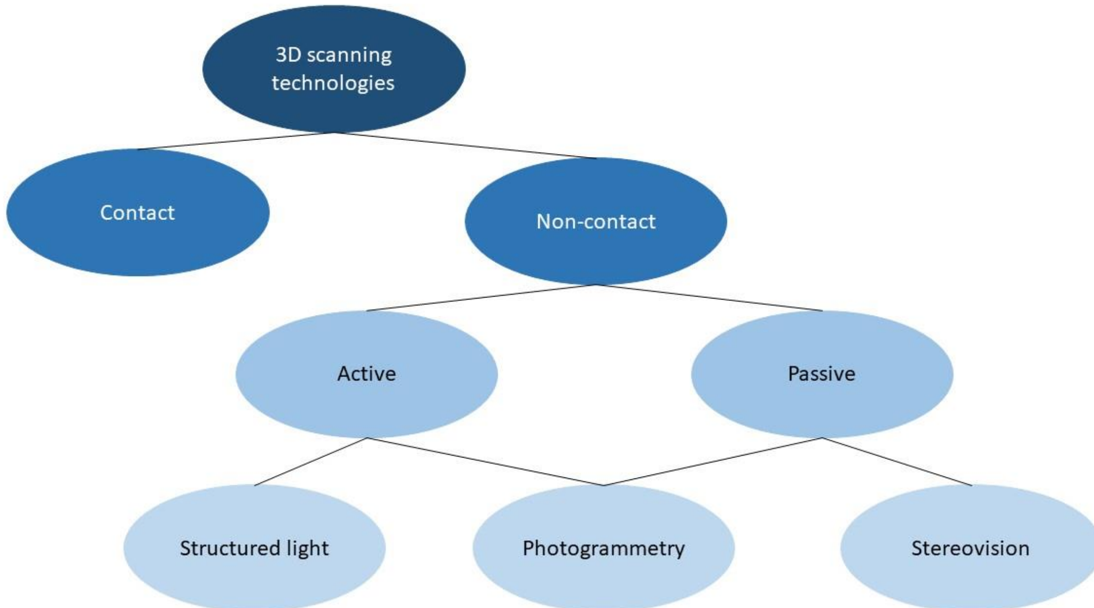

Figure 5: 3D scanning technology classifications

Some important criteria to consider when deciding on a 3D scanner are summarized below [12]. They are rated specifically for the purposes of this research, from 1 being least important to 5 being the most important.

Criterium	Description	Importance (Least 1 - Most 5)
High accuracy	• Helps identify changes in the human body • Replicates an exact 3D model to further help treatment • Provides a holistic view to optimize treatment	5
High speed	• Fast scans easily obtain a clean scan of the body remaining stationary • Comfortable for the patient • Quick turnover	4
Low operational cost	• Efficient for everyday use • Within an affordable price range	5
User friendly	• Simple usability allows for easy integration into the clinical workflow	4
Flexible	• Able to scan entire bodies and small details • Able to be used in various industries, such as entertainment, reverse engineering, 3D visualization, quality inspection, and research	3

Harmless to patient and operator	• Noninvasive to the patients and safe for the operating personnel to use	5
Complex geometry	• System is able to handle potentially complex shapes, such as the breast	5

In the case of researching 3D breast imaging and its use in clinics, certain characteristics were prioritized and ranked. Essentially, the most desirable criteria considered for this research were a system that is easy to use, low cost, provides 3D visualization, and accurate metrics of complex geometry.

As seen in Figure 7, approved 3D scanners that are currently being used in Dutch clinics include the Artec Eva (Artec, Luxembourg) and Vectra XT (Canfield Imaging Systems, Canfield, OH) [17]. A summary of the systems specifications can be found in Table 1, while the details will be discussed further in this section. The Artec Eva is a handheld scanning device with three cameras, and uses fringe projection of structured light to make quick, textured 3D models of medium sized objects, such as a human bust, to large objects, such as a motorcycle exhaust system [18]. It is used on the patient by moving the scanner manually around the area of interest. The Vectra XT setup has three pods with a total of six cameras, which cover 180° field of view. Since it uses multiple cameras at known positions and ambient light, the 3D scanning technology it uses is passive photogrammetry. In a study of the accuracy of the Vectra M3, which is a similar system to the Vectra XT with more focus on facial scanning, the results indicated that the mean distance between the Vectra scan and the highest resolution scanner ranged from 1.1 mm to 4.29mm [14]. Another study of the Vectra XT measuring breast volume accuracy determined an average underestimation of 2.2% of the true volumes smaller than 300 cc [1]. The cost of the Artec Eva is about €13,700 and the Vectra is about €40,000 [17, 18]. Although the Vectra system costs more than the Artec Eva, various studies have shown that it has a lower resolution [14]. However, acquiring images using the Vectra system is a lot easier since it is not handheld like the Artec Eva. Due to the low resolution models produced by these systems, it is therefore desirable to explore other options with possibly better results.

Figure 6: Vectra XT scanner (left) and Artec Eva handheld scanner (right)

The iPhone X is the experimental method for 3D scanning. The iPhone X and following models all use a new front facing camera system called the TrueDepth camera. Figure 8 illustrates all of the components of the iPhone X camera that allow TrueDepth to function [4]. These components are responsible for capturing 3D information for the Face ID unlocking functionality. Figure 8 illustrates the FaceID process, in which a face is detected, an image is taken with the infrared (IR) camera, and dots are projected for depth perspective. The infrared dot projector projects over 30,000 dots in a pattern onto the object, and a photograph is taken by the camera for analysis [19]. The proximity sensor detects that the user is close enough to activate Face ID, and the ambient light sensor helps set output light levels. The flood illuminator adds more infrared light if needed, and the infrared camera picks up skin features to ensure that masks cannot mislead the system. The cost is around €600, which is significantly cheaper than current 3D scanning systems. Using the TrueDepth camera system, an application called Heges was developed, and has proved to take high resolution 3D images. Additionally, the application prioritizes privacy so that data is only shared when the user chooses to upload the images, making this application medically compliant with privacy regulations. The models produced by iPhone X display a comparable quality to current systems being used in hospitals and research; therefore it is worth exploring its capabilities.

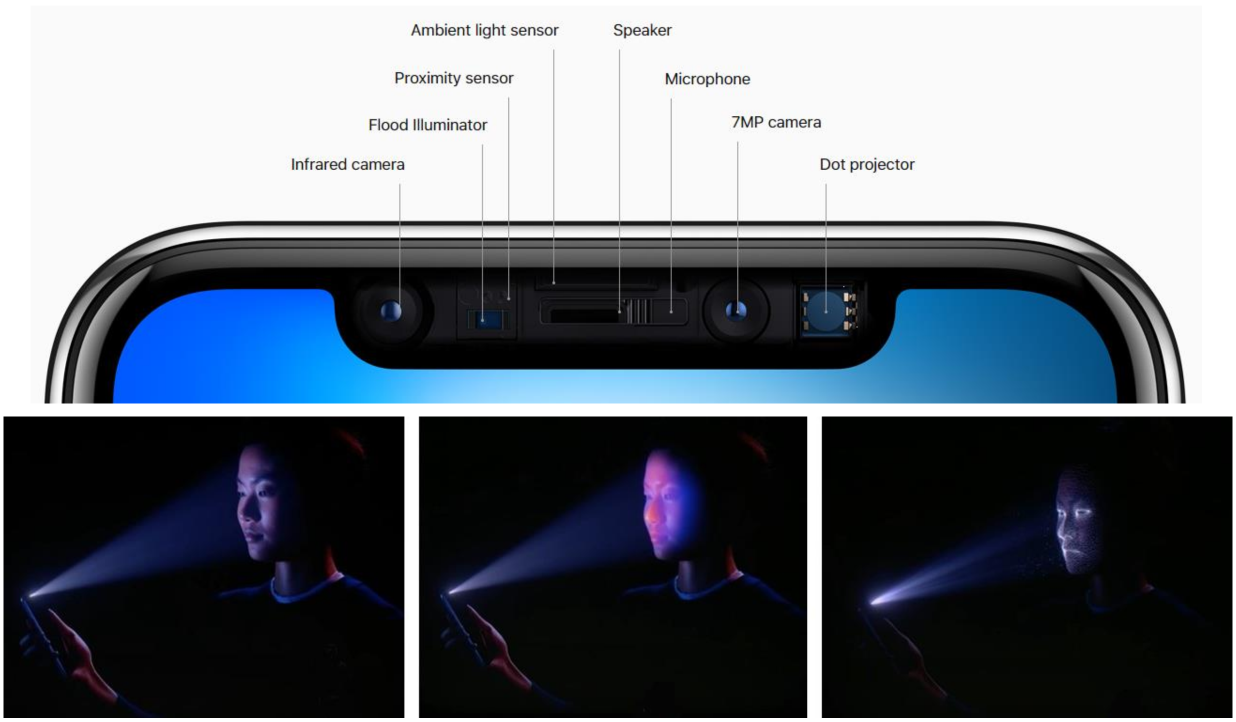

Figure 7: iPhone X TrueDepth camera components (top) [4], face detection, IR, and dot projection for Face ID (bottom)

Product	iPhone X	Vectra XT	Artec Eva
Working principle	Structured light	Passive photogrammetry	Structured light
Coverage	~180 degree Face, torso, parts of the body	Volume (mm): 600x550x350 Face to body	FOV (mm): 536x371 Starting from 10cm
Capture speed	Real time	3.5 ms	16 frames per second
Processing speed	Real time	~80 seconds	2 million points per second
Cost	€600	€40,000	€13,700
Hardware	iPhone components: IR camera, flood illuminator, proximity sensor, ambient light sensor, 7MP camera, dot projector	3 pods, floor stand with motor to raise and adjust to patient height, 36MP color texture	Handheld device

	Tripod, laptop for post processing		
Portable	Yes	No	Yes
Resolution	0.5mm-3.0mm	1.2mm	0.5mm
Accuracy	0.5mm [4]	0.1mm [16]	0.1mm [18]

Table 1: Table of 3D surface imaging systems used for this research

2.2 Mesh Processing Software Packages

After an object is scanned by a 3D scanner, a mesh of the object is produced. A mesh consists of point clouds that describe the individual points in 3D coordinate space. These point clouds are then converted to create a triangle mesh model of the object as shown in Figure 9. The obtained mesh usually requires cleaning up using mesh processing software. The raw mesh contains unnecessary data that will need to be deleted, so it does not interfere with the measurements (Figure 9). Additionally, depending on the 3D scanner, it could be possible that the scale of the mesh is adjusted upon import. It is important to ensure that the digital measurements match the real measurements. Therefore, adjusting the scale of the import can be accomplished using mesh processing software. To identify if this step is necessary, an object with known measurements is used to run a validation test on the equipment. Other important factors to consider are the ability of the software to import and/or export different file types, such as OBJ, Polygon File Format (PLY), and Standard Triangle Language (STL). These are the main file types that are used when working with 3D models. The main benefit of using STL files is its universal recognition, which ensures compatibility with most 3D processing software. This file type is also smaller and makes processing much faster. The downside to using STL files is that it contains no color or texture information. This is where OBJ and PLY file types prove to be more helpful, since they are able to store details such as color and texture. Finally, a large part of processing meshes is ensuring that the model is “watertight”, meaning that the mesh contains no openings and is free of holes, as seen in Figure 10. This is most important for 3D printing the object, but also required for the built-in functions that calculate volumes. Therefore, the desired qualities of a mesh processing software are:

Editing	Shape mesh, align meshes, make watertight, scale mesh
Cleaning	Remove noise
Healing	Close holes
Inspecting	Measurements, check for holes
Converting	Import/export OBJ, PLY, and STL files

The following sections will describe the interfaces, strengths, and weaknesses of the various mesh processing software that were explored for this research.

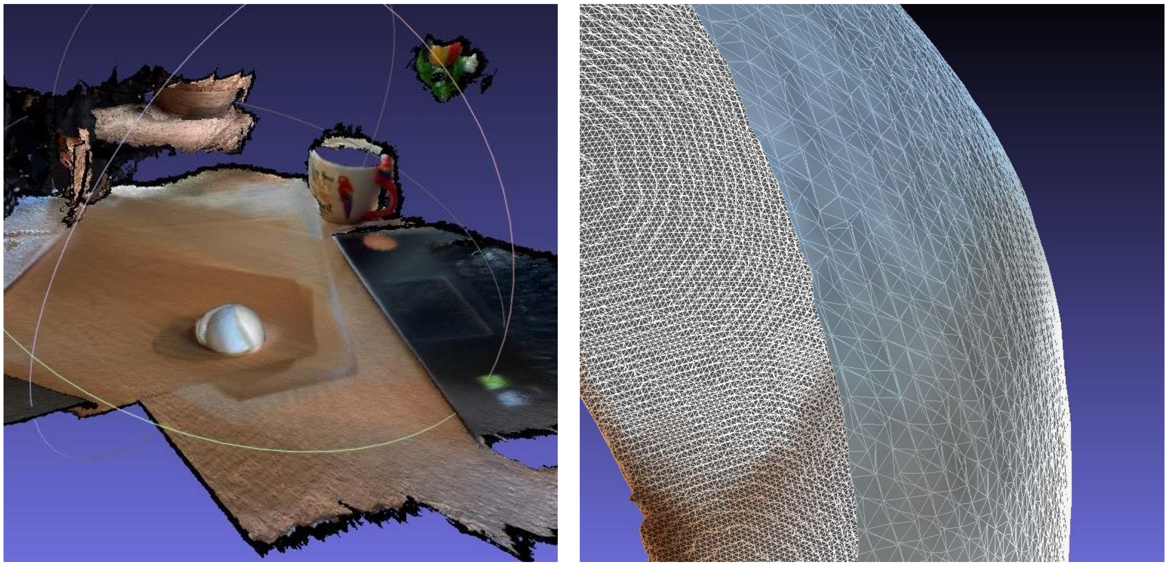

Figure 8: Using Meshlab software, raw unedited mesh of a 3D scan of the phantom (left) includes irrelevant data, and a close up of the triangle mesh illustrating the triangulated point clouds (right)

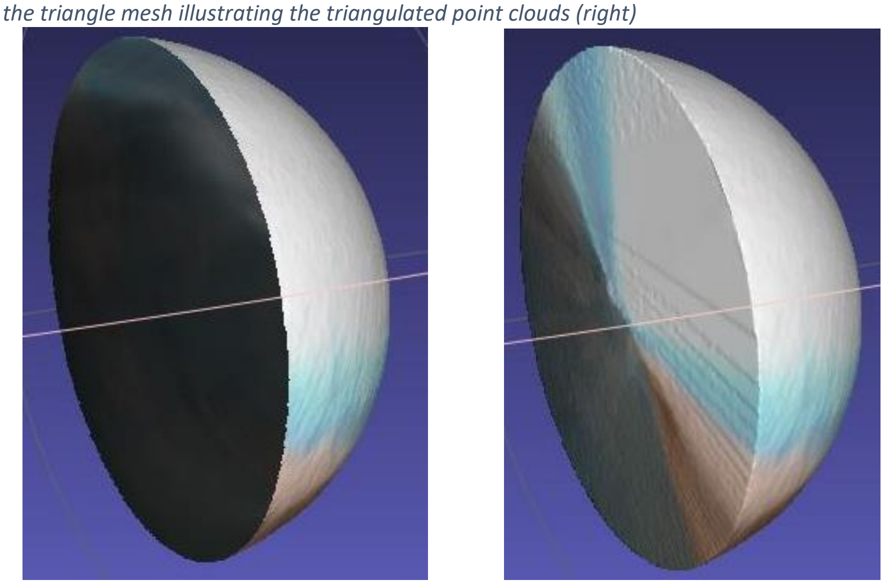

Figure 9: Illustration of a mesh that is not watertight (left), and the same post processed mesh which is now watertight (right)

2.2.1 Meshlab

Meshlab (ISTI-CNR, Pisa, Italy) is an open source software for processing and editing 3D triangular meshes. It was developed by the ISTI-CNR research center in Italy [20]. It contains tools that help with editing, cleaning, healing, inspecting, rendering, texturing, and converting meshes. For this project, Meshlab was especially useful for aligning and editing meshes, as well as obtaining volume measurements. However, the mesh needs to be watertight before being able to obtain volume, which was difficult to do in Meshlab. Additionally, there were issues with Meshlab crashing at unexpected times, resulting in losing the edited data.

2.2.2 Meshmixer

Meshmixer (Autodesk Inc., San Rafael, California) is another open source software useful for cleaning, designing, and printing 3D triangle meshes. It imports meshes, and works as "clay-modeling" for manipulating the surface of the mesh. The main benefit of Meshmixer is how easily it allows for mixing of meshes, resizing them, and making them watertight. Additionally, it contains a useful tool that reports if the mesh has any holes, because there are some cases in which the holes are not visible.

2.2.3 GOM Inspect

GOM Inspect (Zeiss Group, Oberkochen, Germany) is a 3D mesh and CAD analysis software currently used in product development, quality control, and production [21]. This program is capable of importing and exporting standard 3D file formats, and performs 3D mesh processes, such as smoothing, thinning, refining, aligning, and hole filling. GOM Inspect is also able to determine volumes of a mesh, and does not require a watertight mesh to do so. However, this may affect the accuracy of the results so it is not recommended. The basic package is free, but there is also GOM Inspect Professional which offers additional functions. For this research, the GOM Inspect basic package is sufficient to extract volume measurements. The downside is that this software is the most complicated to learn, and the tutorials available are not applicable to the needs of this project. The software also contains functions to fill holes and align meshes; however, there were many errors and difficulties when attempting to use those functionalities. Additionally, to complete some functions that are built into the professional version, workarounds will need to be ascertained on the free version.

2.2.4 D2P

DICOM-to-print or D2P (3D Systems, Rock Hill, South Carolina) is a 3D modeling system that focuses on creating 3D models of DICOM images, and preparing them for 3D printing. DICOM is a file type that stores patient data along with their medical information, such as ultrasound, MRI, or CT images. Although the software was intended to be use for medical applications, there were limitations in editing the mesh and no possible way to calculate volume. Since it is not possible to calculate volumes or edit the mesh, this application was not useful for this project.

2.2.5 Blender

Blender (Blender Foundation, Amsterdam, Netherlands) is an open source computer graphics software that is available for free, and used to create visual effects, animated films, 3D printed models, motion graphics, and computer games [22]. The Blender Foundation is non-profit organization in Amsterdam that maintains development of Blender, and continue to provide access to 3D technology worldwide. This is a very powerful tool, that given enough time and experience, can be very effective in processing 3D meshes in the clinical field. Additionally, it can provide some measurements with a click of a button, including volume and surface area.

Table 2 provides a summary of the previously mentioned software, and their ability to perform the desired functions mentioned in Section 2.2 Mesh Processing Software Packages. Given these strengths and weaknesses, Meshlab, Meshmixer, and Blender were chosen for this research. Initially GOM Inspect was thought to be useful considering its capabilities; however, the difficult learning curve, limited resources, and unhelpful support tools ultimately made it irrelevant for the specific needs of this research.

	Meshlab	**Meshmixer**	**GOM Inspect**	**D2P**	**Blender**
Editing	✓	✓	✓	✗	✓
Cleaning	✓	✓	✓	✓	✓
Healing	✓	✓	✓	✓	✓

Inspecting	✓	×	✓	×	✓
Converting	✓	✓	✓	×	✓
Availability	Free	Free	Free (Standard) Paid (Professional)	Paid	Free
Simplicity	Easy	Easy	Difficult	Easy	Difficult
Support	Video tutorials	Support forum	Manuals, tutorial, support forum	Tutorials	Video tutorials, books, manuals, support forums

Table 2: Summary of the capabilities of the available 3D processing packages

2.3 Segmentation methods

The breast measurements will be divided into two steps. The first step will be to determine the breast boundaries. The boundaries will significantly influence the volume measurements of the breast, since an excess of the surrounding area can be included. There are multiple theories on what the ideal breast boundaries consist of, and these ideas are consolidated and described in this paper below. The second step consists of using a combination of 3D software packages to apply the determined breast boundaries to the meshes. This will allow us to obtain the isolated model that is needed for volume measurements.

2.3.1 Determining breast boundaries

In the study done by Hyun-Young Lee et al, they scanned 37 womens' breasts using phase shifting moiré, and determined a measurement protocol throughout the experiment [8]. The borderline of the breast was found by using the folding line method. This method defines the breast outline by obtaining the line formed when the breast is pushed upward and inward, thereby forming the folding line. The upward and inward breast outlines can be seen in Figure 12 [8]. Due to the fact that the skin surface and the mammary gland forms a tight interconnection, the position of the folding line on the skin surface does not change when there are no forces on the breast [8]. The outer borderline of the breast is obtained by having the subject pose with their hand on their waist, as shown in Figure 11 [8]. Posing in this manner emphasizes the border of the skin making it easier to define.

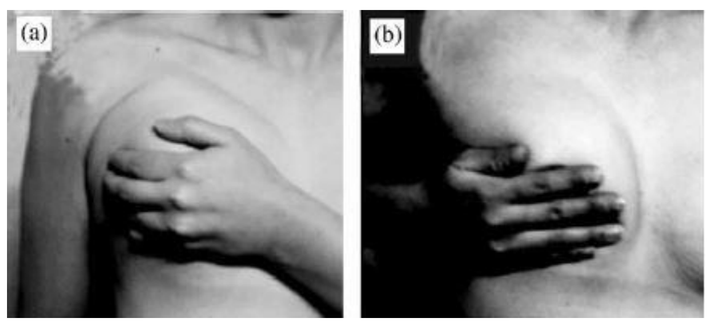

Figure 11: Defining breast outline (a) upward pushing, (b) inward pushing

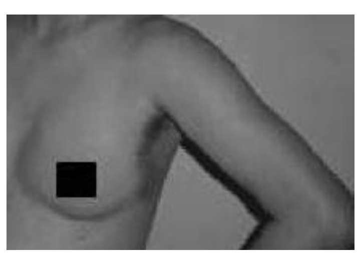

Figure 10: Patient stance position for defining the outer border of the breast

Finally, when calculating the breast volume, the breast borderline was isolated, separated from the bony thorax, and filled at the base, as indicated in Figure 14 [8]. The shape of the base that is used, such as a flat or curved base, can noticeably affect the measured volume. Additionally, the lower breast curve is not symmetrical. Therefore, as shown in Figure 13, the lower breast curve was divided it into two separate regions: 1) outer breast curve (OBC) going from the outer breast point (OBP) to the bottom breast point (BBP), and 2) inner breast curve (IBC) going from the BBP to the inner breast point (IBP). This shows the placement of these landmarks and curves for better visualization. Then a new parameter, the global average radius of curvature, was used as the bottom breast curve line.

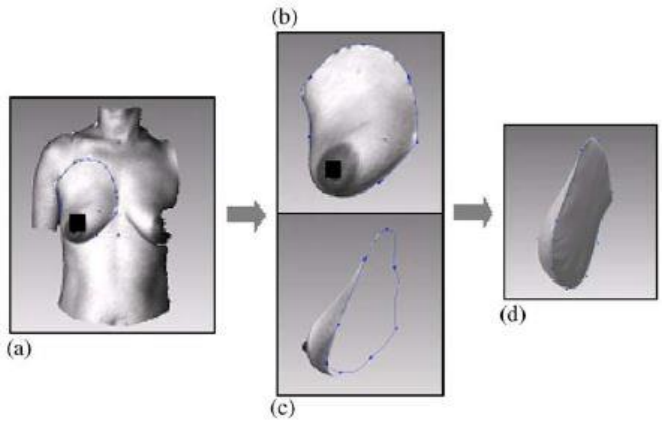

Figure 13: Isolated breast for breast volume calculation (a) defined breast borderline, (b) front view isolated breast, (c) side view isolated breast, (d) isolated breast filled at base

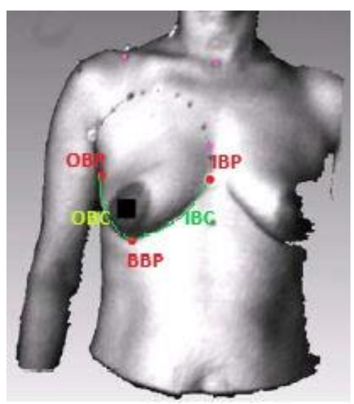

Figure 12: Bottom breast curve diagram, from left to right: outer breast point (OBP), outer breast curve (OBC), bottom breast point (BBP), inner breast curve (IBC), and inner breast point (IBP)

Shown in Figure 15 is a top view of the bottom breast curve points. It is clear from this perspective that there is a much larger difference in the Z-direction between the OBP and IBP, and therefore the boundaries should reflect that. A precise definition of this curvature will result in a more accurate calculation of the volume.

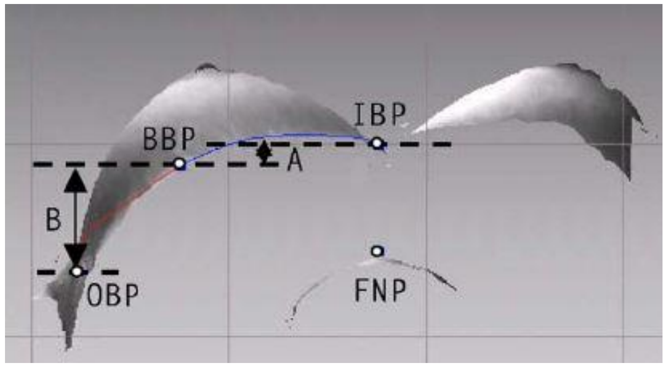

Figure 14: Bottom breast curve points from a top view showing the difference in the Z-direction between the OBP and IBP [8]

In the paper written by Kovacs et al, a linear laser scanner was used on a dummy model and human test subjects to obtain a 3D image of the breast region [2]. For the dummy model, the breast region was marked using the mouse cursor as shown in Figure 16. This mark was made 1 cm below to sternal notch, extending down the medial breast fold, to the submammary fold, along the bottom of the breast fold, continuing up the pectoral muscle, and ending 1 cm below the clavicle [2]. The demarcation of the breast on the dummy model is illustrated in Figure 16a [2]. Raindrop Geomatic software algorithms were used to separate the marked area, and compute the surface to be filled (Figure 16b, Figure 16c) [2]. The corresponding area was subtracted to obtain a closed volume of the breast (Figure 16e) [2].

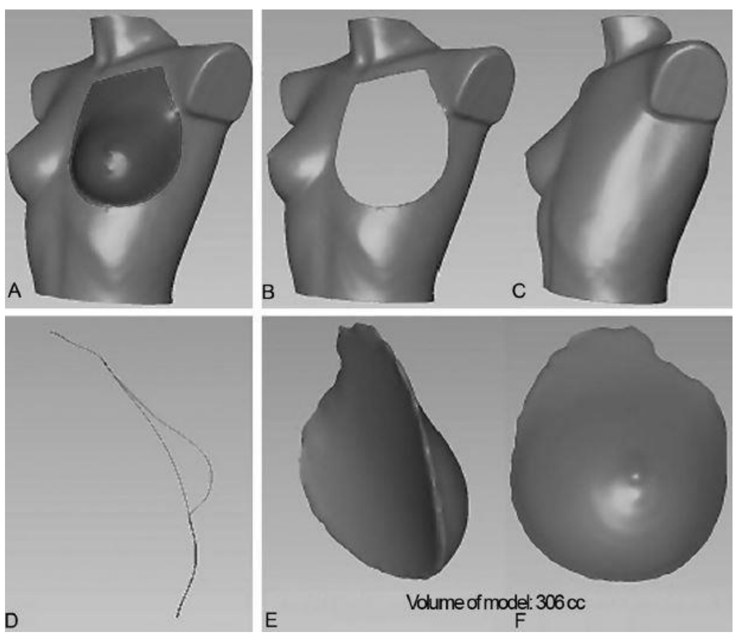

Figure 15: Defined breast boundary of male mannequin with breast prosthetic attachment [2]

For the human test subjects, the folding line method was used to identify the breast border. An MRI was used to determine the chest wall curvature, and a 3D model of the thorax was created by using Raindrop Geomagic Qualify 7 Software. The MRI image and 3D model can be seen in Figure 17.

In the study done by Choppin et al., they utilized a low-cost scanning system of a mannequin to develop an algorithm capable of calculating breast volume [5]. The model was scanned using Microsoft Kinect depth cameras, oriented on the left, right, and bottom at a known distance of 0.7 m. The model was a male mannequin with a prosthetic breast attachment. The breast boundary defined was based on the previous paper by Kovacs. Based on this model, 7 points were chosen to help define the breast region and joined together to form the boundary, as shown in Figure 18 [5].

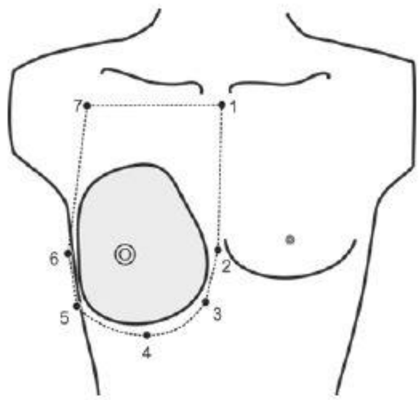

Figure 17: The points of interests defining the breast region [5]

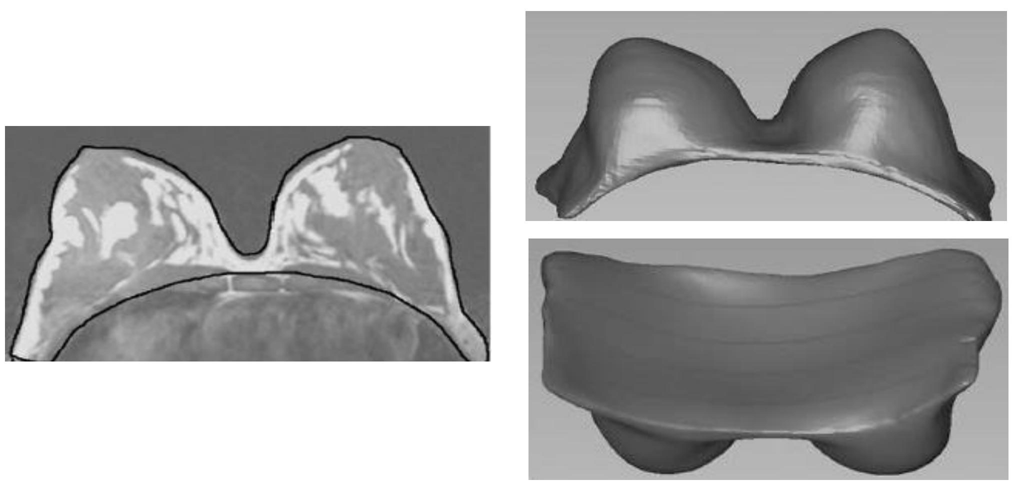

Figure 16: Chest wall curvature determined by MRI (left) and the 3D model thorax reconstruction (right)

These points are labeled as the following [5]:

Point	Location
1. Sternal notch	Visible dip at the base of the neck between the clavicles
2. Medial breast	Point in line with the nipple, 1-2 cm from the middle extent of the breast
3. Medial infra mammary fold (IMF)	Point 1-2 cm from the middle extent of the IMF
4. Bottom IMF	Point 1-2 cm from the bottom of the IMF

5. Lateral IMF	Point 1-2 cm from the outer extent of the IMF
6. Lateral breast	Point in line with the nipple, from the outer extent of the breast
7. Clavicle	Point near the outer extent of the clavicle, same height as point 1

Once the dots were connected, the breast was successfully isolated from the torso. To close isolated breast volume, the chest surface was recreated by using Coons patch [5]. Coons patch is defined for boundaries composed of four curves, in this case, the contours of the isolated breast.

The study done by O'Connell et al. validated the shape and symmetry of the Vectra XT imaging system breast volume measurements [1]. Measurements were taken on breast phantom models varying from 100 to 1000 cc models, as well as 16 patients for *in vivo* reproducibility. The initial attempts of placing landmarks, built-in software, and marking the ROI by eye, resulted in too much variation that affected the reproducibility [1]. A specific protocol was developed to use the Vectra Analysis Module (VAM) software to calculate the breast volume. As shown in Figure 19, a grid was placed on the image in which each box measured 2 cm, and the y axis was positioned midline such that it intersected with the sternal notch. The ROI, highlighted in green in Figure 19, was identified around the perimeter of the breast with the following specifications [1]:

1. Along the y axis midline, one square below the sternal notch extending to one square below the middle IMF.
2. Moving horizontally across, one square below the IMF, parallel to the bottom curve of the breast.
3. Moving vertically up to the underarm.
4. Moving inward and upward to one square below the clavicle, which is horizontal to the starting point at the sternal notch.

The final breast volume measurements were taken using the Vectra XT imaging system. There were no additional methods used to recreate the chest wall, so the measurements rely heavily on assumptions of the depth and curvature of the chest wall made by the Vectra system.

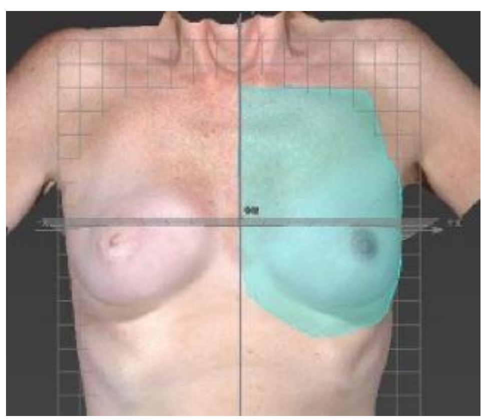

Figure 18: Method to measure volume of the breast using Vectra-XT 3D-SI [1]

These different methods of isolating the breast from the chest wall can influence the final breast volume measurements and the accuracy, so it is important to take into consideration the current methods that are used and how they influence the final results. In Table 3, the previously described methods are consolidated for an overall viewpoint. It is apparent that most of the studies involve landmarks at the clavicle, sternal notch, and IMF areas, and outline borders using those points. The variation comes from the curvature of the breast outline and the shape of the torso reconstruction.

Author	Method	Test subject
Hyun-Young Lee et al.	1. Upper breast border identified by folding line method 2. Outer border by having patient pose with hand on waist 3. Bottom breast curve divided into outer and inner breast curve 4. Segmented breast filled at base	Human
Kovacs et al.	1. Dummy model: breast region starts 1 cm below sternal notch, down medial breast fold to submammary fold, along the bottom of the breast fold, and up pectoral muscle ending 1 cm below clavicle 2. Human models: Folding line method for breast border 3. MRI to determine chest wall curvature	Dummy and human
Choppin et al.	1. Similar to Kovacs et al dummy model 2. Coons patch to recreate chest wall	Dummy
O'connell et al.	1. 2 cm grid superimposed on image 2. ROI is selected: beginning 2 cm below sternal notch extending down to 2 cm below middle IMF, across the bottom breast 2 cm below IMF curve, upward towards the underarm, and inward and upward to 2 cm below clavicle	Human

Table 3: Summary of breast segmenting methods described from previous papers

For this study, the landmarks marked on the mannequin corresponded to the points required for the Vectra device to obtain measurements. Figure 20 shows where the specific landmarks were drawn on the mannequin. Similar to the previously mentioned studies, there are landmarks at the sternal notch and IMF curve. These points include the sternal notch, midclavicular lines, the nipples, the areola borders, and the bottom, lateral, and medial IMF. Using these landmarks, it is possible to define the breast boundaries and segment the breast from the torso for volume measurements. Due to this study being done with the availability of the Vectra XT, these landmarks will be used in order to determine the breast boundaries and segmentation.

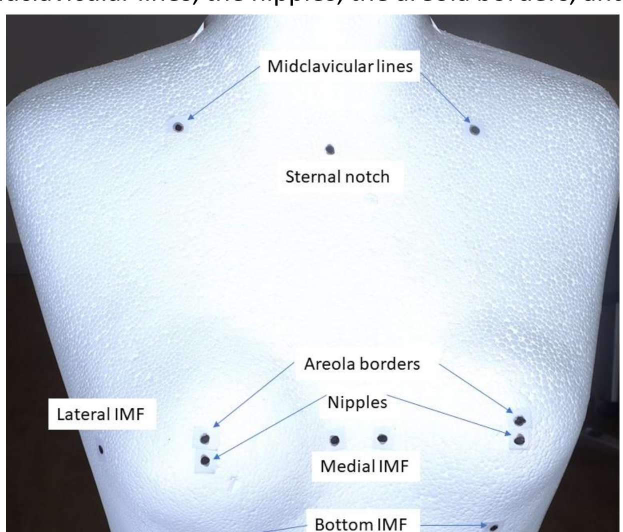

Figure 19: Mannequin breast landmark anatomy for Vectra

2.3.2 Software application of breast boundaries to 3D mesh models

It is important to explore the strengths and weaknesses of the different software packages, since there are various ways the 3D meshes can be processed and isolated. The following requirements remain in processing the breast models:

- Remove background noise
- Align meshes to ensure similar positioning of models
- Scale mesh
- Close holes
- Recreate the chest wall, thereby closing the mesh to be watertight
- Obtain volume measurements
- Export to STL, PLY, or OBJ files for 3D digital visualization or 3D printing

The goal is to find a software package that performs all of the tasks in a streamlined manner, to easily use in a clinical setting. It is also important to verify each step, and validate for any potential errors that may occur with the final measurements. Furthermore, scans of the same objects will be done multiple times to test for reproducibility. Figure 21 outlines the necessary steps after the object is scanned by the 3D scanner, and the packages that can perform those steps. In this research process, it was important to ascertain a process that would ensure that the applications would not crash or slow down. Therefore, the figure illustrates the specified order that was found to be the most efficient method of handling the mesh data. Each step also lists the software applications that are capable of completing the task.

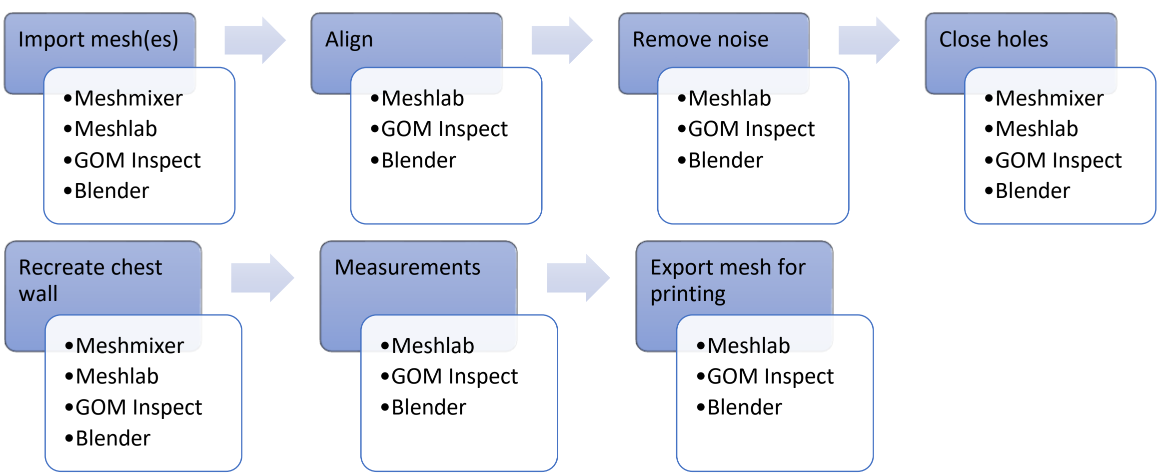

Figure 20: Illustration of the steps to process the 3D mesh and the capable software

An important consideration when importing the meshes is whether to use the STL or PLY/OBJ file types. Although STL files are faster to process, the color and texture information provided by PLY/OBJ files makes processing the mesh more intuitive. With the color information, it is possible to visualize the relevant landmarks needed to accurately align and segment the mesh. Also from various trials, it was shown that importing STL files into GOM Inspect produces an error when measuring for volume. This error does not appear when using PLY file types. Due to these issues in using STL files, PLY file types were used in the remainder of the research.

2.4 3D Phantoms

The general goal of this project is to have a 3D model that accurate allows representative measurements to be obtained. These measurements should also be validated against the measurements of the original object, and reproduced with minimal error. This study specifically focuses on the 3D scan of the chest. Choosing a viable 3D object to scan for both scenarios should be considered carefully. There are many breast phantoms to choose from. Some phantoms are designed to mimic the breast tissue and density, whereas others mimic the anthropomorphic properties of the breast. Taking into consideration the time and financial limitations, the most important aspects of the breast phantoms are: (1) it consists of a complex shape that mimics the breast, and (2) calculating the actual volume is possible for comparison to the 3D scan data. Figure 22 depicts all of the phantoms that were used for this study.

The simple shaped phantoms that were used for the validation of the methods were a half globe and a styrofoam ball cut in half. Both items were used in the assumption that they are halves of a perfect sphere. With this assumption, it is easy to measure and calculate the dimensions of the phantoms, such as volume, surface area, diameter, and base circumference. Since the built-in volume function in Meshlab does not provide units for the measurements, these simple shaped phantoms were needed in order to understand the numbers that were obtained. Since these objects are easy to measure in real life, they can be used for validation. The numerical results obtained from the scanned phantom can then be compared to the actual measurements. The styrofoam ball is already solidified and ready to be scanned; however the size was small, so the half globe was used for larger scans. To make the half globe model watertight, a cardboard piece was cut out to fit at the base, and the entire object was covered in cellophane to prevent any small water leaks.

For a more complex phantom, a torso of a mannequin with breast attachments made of a moldable material, such as dough, was used. The volumes of the dough are already known, and can be compared to the measurements obtained from the software packages. Scans and known volumes of these models were provided by Amsterdam UMC.

Figure 21: Styrofoam half sphere (left), half globe (middle), mannequin with breast attachments (right)

3. Procedure

3.1 Calculating actual measurements

Using the half spherical validation objects, which will be referred to as the half globe and styrofoam, basic measuring devices, and simple geometry, we are able to acquire the actual specifications of the objects. The base circumference of the dome and the diameter measurements were gathered using a tape measure and calipers. Knowing these variables, it is possible to calculate the actual volume and surface area. Additionally, since two separate variables were retrieved with slight inconsistencies, two sets were calculated. This means there was a calculated volume with respect to the measured radius (V(r)), and a calculated volume with respect to the measured base circumference (V(C)). The volume with respect to the radius and circumference are described by equation (1) and (2).

$$(1)\ V(r) = \frac{2}{3}\pi r^3$$

$$(2)\ r = \frac{C}{2\pi}, therefore\ V(C) = \frac{C^3}{12\pi^2}$$

Furthermore, for comparison, the volume of the test objects was measured multiple times using Archimedes water displacement principle (n=6). A water-filled container was placed inside of another container to catch the displaced water when the object is placed in the first filled container. Some force was required to fully submerge the objects, so a flat board was used to push the object into the water. The displaced water is then weighed on a scale. Under the assumption that 1 gram=1 cc of water, we can measure the volume through water displacement.

3.2 Obtaining 3D scans

The half globe validation object was first sealed by creating a flat base out of cardboard, and wrapped in cellophane prior to scanning. This maintains the consistency of the results between the scan and the water displacement tests. After verifying that the objects were ready for scanning, they were placed on the center of a table to be scanned by the iPhone, as shown in Figure 23. Since the iPhone Heges application only works with the front facing camera, the scanning process needs to be performed slowly and carefully to ensure that the object of interest remains in view. This was repeated multiple times to obtain 5 meshes of each object, with a total of 10 meshes.

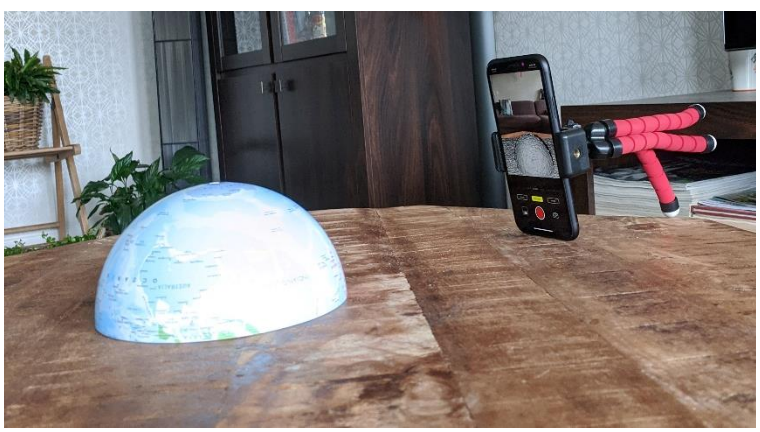

Figure 22: 3D scanning set up of the half globe

The scans of the breast phantoms were shared by the group at Amsterdam UMC. The 3 sets of scans were obtained by using the iPhone, Vectra, and Eva scanners. The iPhone was placed on a tripod with a moving arm to help navigate the phone around the mannequin. Shown in Figure 24 is the 75 cc breast phantom mannequin. The mannequin contains the landmarks which correspond to the points of interest, that are needed to obtain measurements by the Vectra and Eva applications. The following scans were given of the mannequin: no breast attachment (0 cc), 75 cc, 100 cc, and 125 cc. The volume measurements refer to the added volume for each breast.

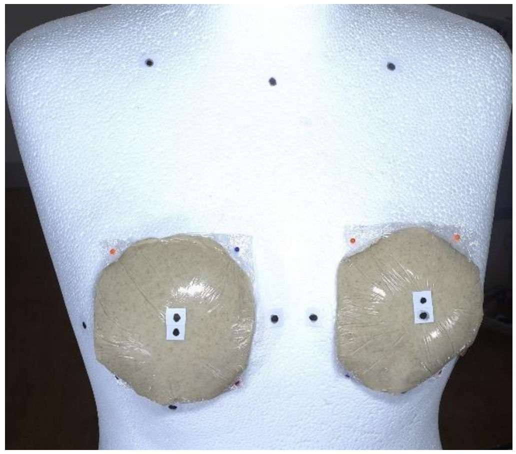

Figure 23: 75cc breast phantom model provided by Amsterdam UMC, containing specific landmarks for Eva and Vectra measurements

3.3 Processing 3D scans

Throughout this research, the mesh was processed in the following way:

1. remove noise
2. align all meshes to the same orientation
3. segment the relevant information
4. reconstruct the bounds to make watertight
5. retrieve measurements

These three applications have proven to be the most sufficient in collaboration with each other: Meshlab, Meshmixer, and Blender. It was possible to use Meshlab for all the steps in processing the 3D scans. The process branches off when making the mesh watertight, as Meshmixer and Blender use a different solidifying process resulting in slightly different volumes. If the mesh is successfully processed and watertight, the volume measurements can be done by using Meshlab and Blender. Note that even though the mesh is made watertight using one application, the measurements made by Meshlab and Blender matched. However, depending on which application was used to make the mesh watertight, the measurements varied. This variation comes from which application was used to solidify the mesh, and not from which application was used to make the measurements. For example, a mesh that was solidified using Meshlab resulted in the same volume measurements when taken with both Meshlab and Blender. Figure 25 is a flowchart of the three different processes that were explored in acquiring the mesh measurements.

For the breast phantom scans provided by Amsterdam UMC, Meshmixer was used to solidify the mesh. This was found to be the simplest method to process the scans, before taking measurements using Meshlab or Blender. With the assumption that the base mesh remains the same across all scans, the volume of the base was subtracted from the 75 cc, 100 cc, and 125 cc. This should provide results of the additional breast volume.

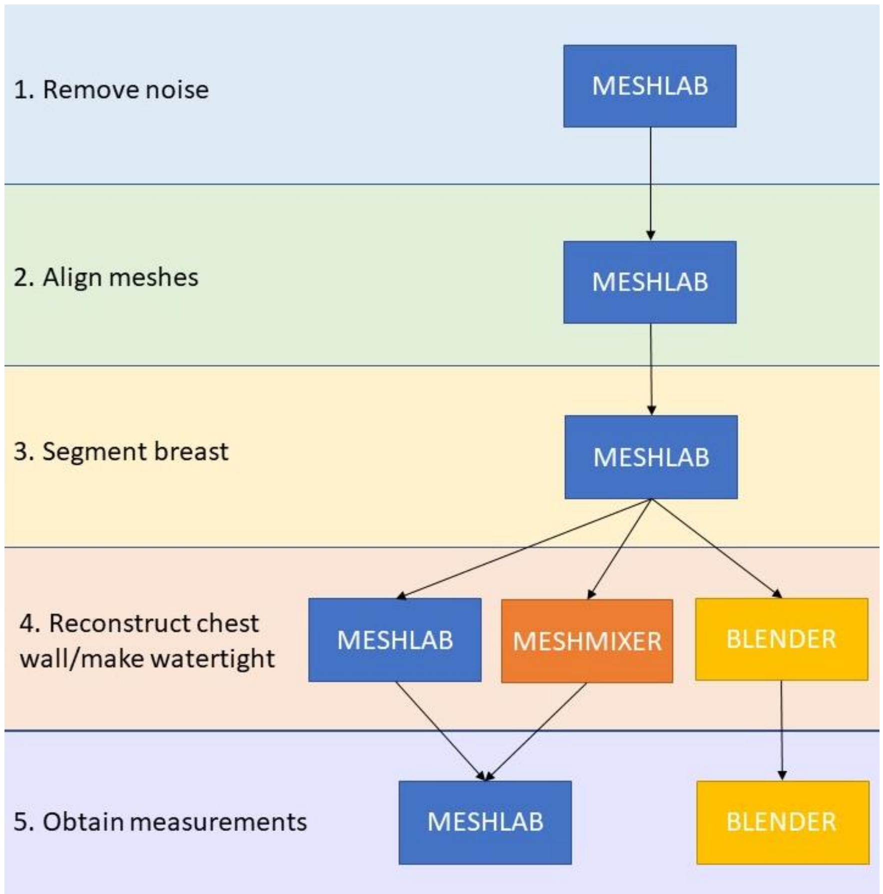

Figure 24: Mesh processing tasks and the useful 3D mesh processing applications

3.3.1 Watertight functions

Depending on the shape, the methods for making a mesh watertight can vary considerably. For Meshlab there is a function called convex hull, which binds all the points in an enclosed volume in the smallest convex set that is contained in the shape. The resulting shape is similar to a rubber band that is stretched around the subset of the perimeter points. For Meshmixer, the watertight function is called "make solid." It closes, in a simple manner, any openings of the shape with a straight plane. Lastly, the function for Blender is called "make manifold," which is the desirable trait in 3D geometry for a watertight mesh. All of these functions use different approaches to creating a watertight mesh. However, for the breast phantom mesh, the Meshlab convex hull method does not work very well, because it adds extra volume to the front, instead of only recreating the thorax wall, as shown in Figure 26. Therefore, the test object meshes were successfully made watertight using all 3 applications, whereas only Meshmixer and Blender were successful in making the breast phantom meshes watertight.

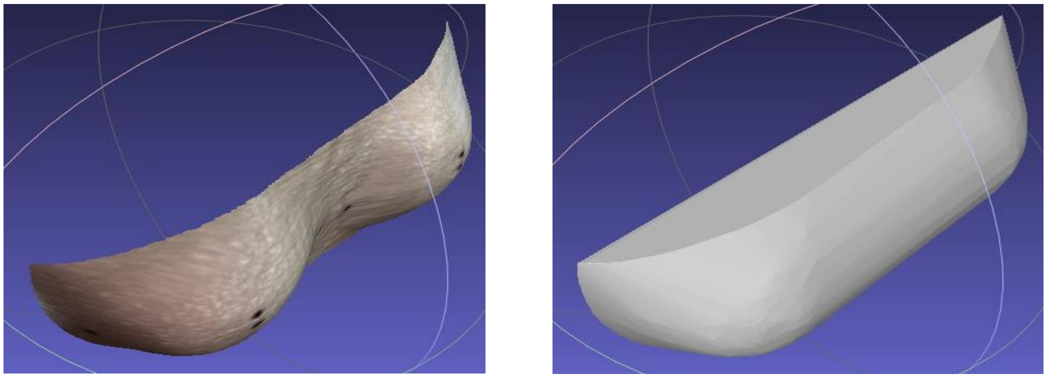

Figure 25: 0 cc breast mesh before convex hull remesh (left) and after convex hull remesh (right)

3.3.2 Rescaling Meshes

An additional step taken for the Vectra and Eva scans was to rescale the mesh. The original, unscaled mesh resulted volumes in the range of cubic meters. This step is recommended any time before the segmentation step, because there are more landmarks available. The length for the x, y, and z direction were taken for the iPhone and Vectra or Eva scans. This information can be used to calculate the scaling coefficient.

4. Results

4.1 Volume of hemispherical test objects

Figure 27 illustrates the following: (1) the circumference measurements of the hemisphere objects, which were taken multiple times (n=10) with a tape measure; (2) the diameter measurements which were measured using calipers and divided by 2 to obtain the radii. The circumference of the objects were divided into 20 points to mark the diameter end points, ensuring that the measured diameter passes through the center. For the styrofoam, the points were 0.9 cm apart, and the half globe points were 2.4 cm apart. The radii and circumference measurements resulted in slightly different calculated volumes V(r) and V(C), respectively. Table 4 shows the average of volume; average surface area A(r) and A(C); standard deviations; and percent error. The volumes have a percent error of 2%, while the area resulted in a percent error of 1%. It is expected that the volume results in a larger error than the area. These values will be used as the gold standard value for comparison to the 3D scans. Table 10 in the Appendix contains the raw data of the radii and circumferences measured, along with the calculated volumes and areas for each measurement.

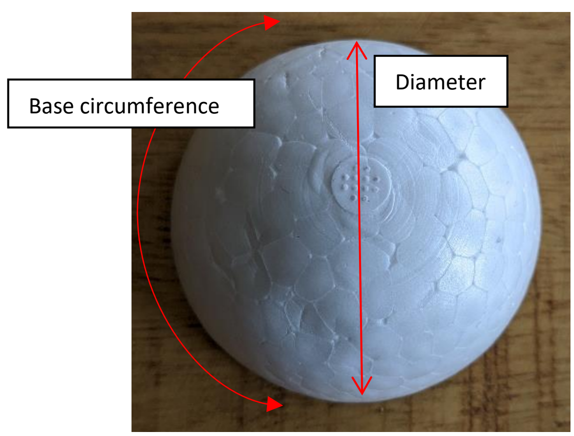

Figure 26: Parameters measured on hemisphere objects (diameter which is 2r and base circumference C)

	n	Half globe	% error	Styrofoam	% error
Average volume (cc)	10	928 ±8.9	2%	63.18 ±0.69	2%
Average area (cm^2)	10	548 ±3.4	1%	91.4 ±0.67	1%

Table 4: Average volume and area of the half globe and styrofoam test objects

Additional volumes of the test objects were obtained using the water displacement method for comparison (n=6). The results of the water displaced volumes are shown below in Table 5. There is a learning curve with the procedure for obtaining the measurements, which started with the styrofoam hemisphere. Therefore, the first measurement appears to be an outlier when compared to the other 5 measurements. This has been omitted from the calculations, so the number of trials for the styrofoam measurements is n=5. The average of the volumes were calculated to be 981 cc and 73 cc for the half globe and styrofoam, respectively. The difference from the gold standard/true value and percent errors were calculated using the true volumes in Table 5.

Water displaced volume (cc)	Half globe (n=6)	Difference from gold standard	% error	Styrofoam (n=5)	Difference from gold standard	% error
1	993	65	7.00%	-	-	-
2	995	67	7.22%	78	15	23.5%
3	978	50	5.39%	73	10	15.5%
4	966	38	4.09%	71	7.8	12.4%
5	972	44	4.74%	74	11	17.1%
6	983	55	5.93%	70	6.8	10.8%
Average	**981**	**53**	**5.73%**	**73**	**10**	**15.9%**
SD	**10.5**			**2.8**		

Table 5: Volumes acquired using water displacement method of the test objects

The iPhone Heges application made a 3D scan of the half globe and the styrofoam 5 times to produce 5 meshes of each object. They were processed in the 3 methods described in Section 3.3 Processing 3D scans. Table 6 below displays the results of each volume measurement, and their averages with their standard deviations. The percent error was obtained by using the volumes from Table 4 as the accepted value. Figure 28 displays a bar graph of the measured volumes by Blender, Meshlab, Meshmixer, and the water displacement method with the true value for the half globe and styrofoam objects. It can be seen that the water displacement method results in an overestimation of the true volume, while the 3D meshes result in an underestimation.

	Blender	% error	Meshlab	% error	Meshmixer	% error
Halfglobe measurements (cc)	**824 ±54**	**11%**	**833 ±53.6**	**10%**	**826 ±52.9**	**11%**
1	776		786		781	
2	753		764		756	
3	821		828		822	
4	890		898		891	
5	878		889		879	
Styrofoam measurements (cc)	**56.9 ±1.21**	**10%**	**58.2 ±1.33**	**7.9%**	**57.2 ±1.33**	**9.47%**
1	57		58		57	
2	58		59		58	
3	57		58		57	
4	58		60		59	
5	55		56		55	

Table 6: Volumes of the test objects obtained from processing the mesh in Blender, Meshlab, and Meshmixer

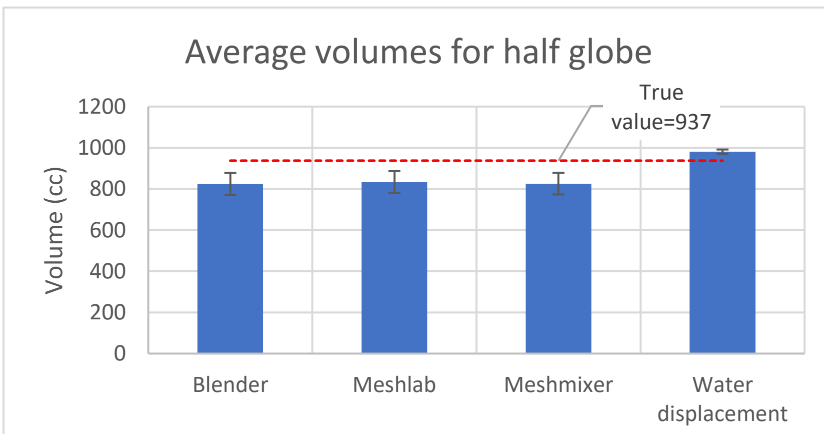

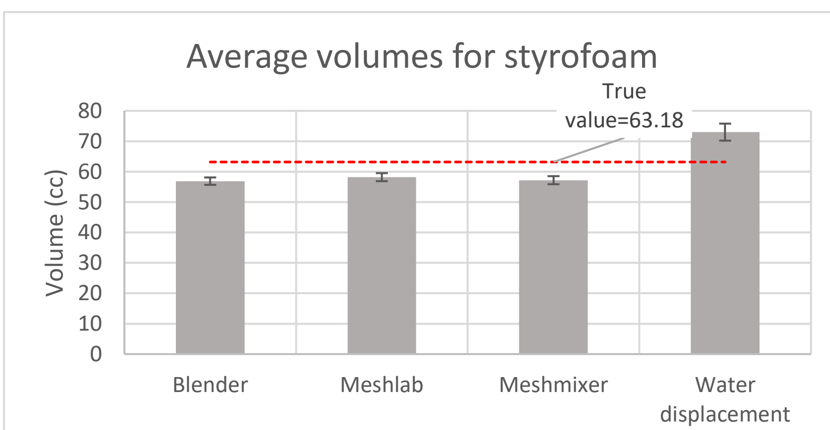

Figure 27: Graph of average volumes and standard deviations of the half globe (top) and styrofoam (bottom) using Blender, Meshlab, Meshmixer, and water displacement method. True value is indicated with the red dotted line.

4.2 Volume of breast phantoms comparing scan methods

The measurements for the breast phantom were iPhone, Vectra, and Eva scans were processed similarly to the test object meshes. The one difference is that only Meshmixer and Blender could be used for solidification. An additional step for the Vectra and Eva scan needed to be taken to rescale the mesh size. In contrast, this rescaling step was not necessary for the iPhone scans. The volumes were measured using Meshlab and Blender, and are shown in Table 7. The base mesh was subtracted from the 75 cc, 100 cc, and 125 cc meshes to provide the difference. In theory, this should provide the volume that was added for each model. The error of these differences was calculated by subtracting the difference and the known volume of the breast phantom (150 cc, 200 cc, and 250 cc). Figure 29 plots the known volumes (blue), the measured volumes obtained from Meshmixer/Meshlab (orange), and Blender (gray).

		Meshmixer /Meshlab (cc)	Difference (cc)	Err	% error	Blender (cc)	Difference (cc)	Err	% error
iPhone	**base (0 cc)**	644	-			744	-		
	75 cc	809	165	15	10%	861	116	-34	22%
	100 cc	1071	427	227	114%	1075	331	131	66%
	125 cc	1113	469	219	87.6%	1135	391	141	56%
Vectra	**base (0 cc)**	916	-			758	-		
	75 cc	1089	173	23	15.3%	946	188	38	25%
	100 cc	1230	314	114	57%	1336	578	378	189%
	125 cc	1279	363	113	45.2%	1282	524	274	110%
Eva	**base (0 cc)**	849	-			771	-		
	75 cc	1047	198	48	32%	1035	264	114	76%
	100 cc	1213	364	164	82%	1157	386	186	93%
	125 cc	1296	447	197	78.8%	1281	510	260	104%

Table 7: Breast phantom measurements obtained from scanning with an iPhone, Vectra, and Eva

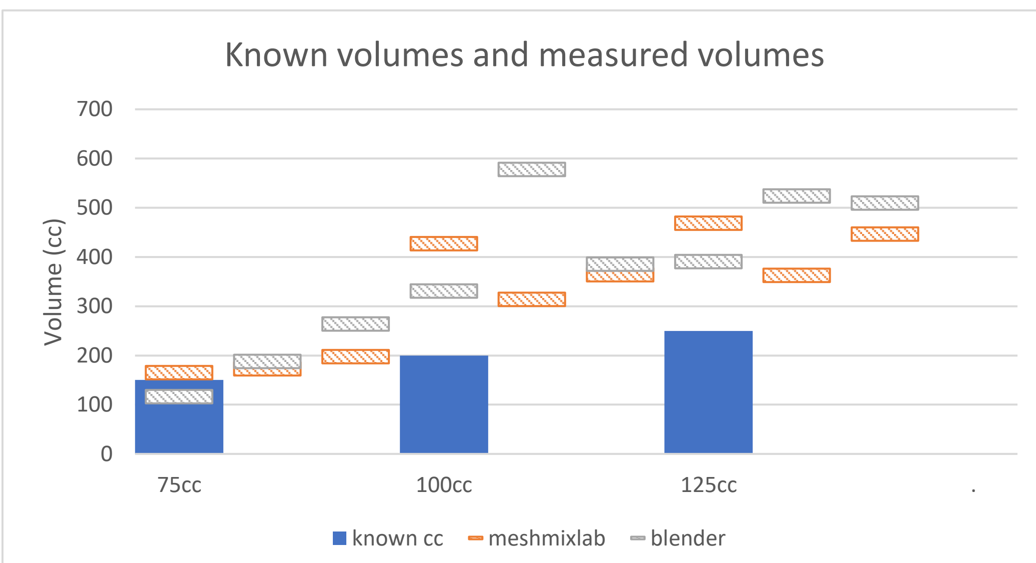

Figure 28: The known volume (blue), measured volumes obtained from Meshmixer/Meshlab (orange), and Blender (gray)

5. Discussion

The overall goal of this study is to explore the capabilities of using an iPhone X to obtain 3D scans, and the accuracy of volume measurements from the iPhone X scans. In the first part of this study, 2 hemisphere models were used as validation of the scanning and mesh processing procedures. This is possible because the volumes of these objects can be physically measure using conventional tools, such as a tape measure and calipers; which are then compared to their digital counterpart. The objects were scanned by the iPhone 3D scanning application called Heges. These scans provide a 3D mesh of the hemisphere, and the background, which is later removed. Using 3D mesh processing software, Meshmixer, Meshlab, and Blender; the noise is removed; object of interest is segmented from the background; and the mesh is made watertight to acquire volume measurements. The specified steps of this process are represented graphically in Figure 21 (located in Section 2.3 Segmentation methods). The final 3D visualized results obtained by the iPhone were validated with the physically measured results.

The second half of the study tested the feasibility of using the validated mesh processing software and iPhone scanner for a clinical application, such as breast volume measurements. In this case, a mannequin was used with different breast prosthesis, 75 cc, 100 cc, and 150 cc. These volumes refer to each breast, therefore, the total breast volume is 150 cc, 200 cc, and 300 cc. Meshes were provided by Amsterdam UMC, and scans were obtained using the iPhone X, Vectra, and Eva scanners. These meshes were processed as illustrated in Figure 25 (Section 3.3 Processing 3D scans), and compared to the true volumes. This information makes it possible to compare the mesh processing methods, and measurements obtained with the various 3D scanners.

5.1 Results

5.1.1 Golden standard/true volume

There is a 1%-2% error with the physically obtained measurements, because identifying the precise center diameter is a manual process. Calipers were used to measure the diameter, however, the small discrepancy can be explained by how tightly the calipers were clamped around the object, which would affect the measurements. Both the styrofoam and half globe objects are slightly malleable, and therefore, it is very easy for the calipers to underestimate the true diameter of the object if clamped too tightly. This was done as carefully as possible, but could account for some of the deviations seen in the millimeter scale. Additionally, when measuring the circumference of the base, it is possible that the thickness of the measuring tape slightly added to the overall circumference. The error for these measurements are small, and thus, it is acceptable to use as the golden standard measurements to validate the digital measurements.

5.1.2 Water displacement method

While acquiring the actual volume of the objects using the Archimedes water displacement method, it resulted in a slightly larger volume than what was calculated. This could be explained by the method used when performing the water displacement. The ideal way to perform the water displacement test is by placing the object in a graduated cylinder; however, there is no graduated cylinder available that is large enough for such an object. A different approach was taken by using a flat board to push down the test object into the water, catching the displaced water, and weighing the displaced water. The flat board that submerged the test object possibly made some contact with the surface of the water and the edge of the bowl. Due to the cohesive properties of water, this could have caused additional water to displace. Taking all of this into consideration, it is possible the most accurate true measurements of the test objects are calculated from measuring the diameter and circumference. Therefore, the half globe and the Styrofoam test objects actual measurements are best represented by the calculated average volume and area values in Table 4 (Section 4.1 Volume of hemispherical test objects).

5.1.3 Comparison of mesh processing software

For the test object measurements taken by the iPhone scan and processed using Meshmixer, Meshlab, and Blender, it is possible to compare the different software to each other. The styrofoam test object resulted in volumes ranging from 56.9 cc-58.2 cc, while the half globe had a larger range from 824 cc-833 cc, due to it being a larger object. There is also a general trend with Blender producing the smallest results, and Meshlab resulting in the largest volume, that is closest to the golden standard value. Comparing the true volumes to those determined using the 3D scans, there is an error ranging from 9%-12% with all the used applications; and the trend appears to be the results of the scans underestimating the true volume. This underestimation could be explained by the 3D mesh processing, since some information is removed during segmentation. Planar selection was used to select the vertices to be separated from the object of interest. It is possible that when segmenting the object from the table it was lying on, a section of the base of the object was removed, because the object vertices lie on a close plane to the table vertices. Selecting vertices for removal is a manual process, and limited to the selection methods available in the software. Some of the other options available included selecting faces by color, non manifold edges/vertices, disconnected components, self intersecting faces, borders, visible points, and problematic faces. However for this shape, using planar selection seemed to be the most efficient method of segmentation. Out of the 3 software packages used for processing 3D meshes, Meshlab seems to show the most potential in volume acquisition, since the results had the smallest error and the entire mesh could be processed within that single application.

5.1.4 Breast phantom scans

There is a clear visual difference between the iPhone, Eva, and Vectra scans, because the Eva scan is capable of delivering a full mesh of the torso, whereas the iPhone and Vectra scans struggle with scanning the back of the model. Nevertheless, for this study, a full 360˚ model of the torso with the back is not necessary since we are only interested in the front volume of the breast and remove the posterior part of the torso during processing. However, despite the meshes being larger and more complete in the Vectra and Eva scans, the total count of vertices and faces is less than the iPhone mesh. This data can be found in Table 11 of the Appendix. In Table 8 below, the mesh density of the base torso is calculated in vertices per surface area (cm^2). These numbers were taken after cleaning the mesh, removing the background noise, and segmenting the same part of the torso for all scans. The surface area of the Vectra model measured to be 106.5 cm^2, and was used to obtain the mesh densities for comparison. This ensures that the same area is being compared. However, it is apparent that although the same area of the mesh was selected, the measured surface area varied for each mesh from 71.64 cm^2-181.7 cm^2. Vectra shows the lowest mesh density of 77.96 v/cm^2, while the iPhone X has the highest mesh density of 1798 v/cm^2. In the images it is also noticeable that the edges in the Vectra scan appear to be more rough, due to the less dense mesh, while the iPhone X contains smoother edges. The smoother mesh allows for better representation of the 3D scan and more control over the segmentation. These densities indicate that the mesh resolution of the Vectra and Eva scans are much lower than the iPhone mesh. Mesh density plays an important role in influencing the measurements, since meshes with large elements would replace curved shapes and details with a flat element. This could change the overall shape of the mesh, so that it does not represent the original model, resulting in inaccurate measurements.

	Selected Vertices	Total Vertices	Surface Area (cm²)	Mesh density (v/cm²)	Mesh Image
Vectra	8304	31622	106.5	77.96	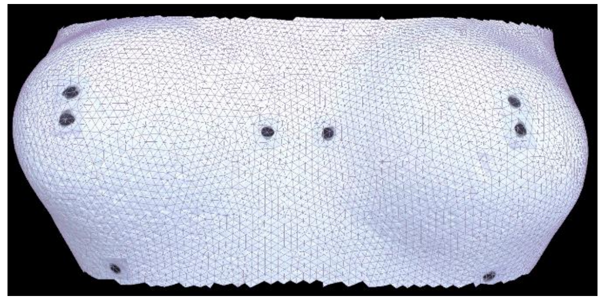
Eva	58894	251355	181.7	553.0	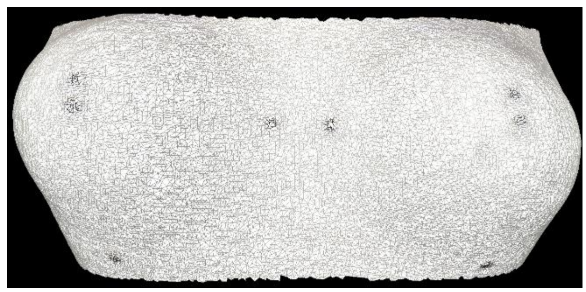
iPhone	191480	549620	71.64	1798	

Table 8: Mesh density of the Vectra, Eva, and iPhone original mesh and the corresponding graphics

Since the original mesh measurements were uploaded into Meshlab and Blender in the magnitude of meters, the Vectra and Eva scans were rescaled to be smaller. Since the validation of the previous iPhone hemisphere scans shows that rescaling is not necessary, the iPhone scans were used to determine the scaling factor for the Vectra and Eva scans. The method for scaling was to measure the length in the x, y, and z, direction of the Vectra (x_V, y_V, z_V) and Eva (x_E, y_E, z_E) meshes, and scaling them to the x, y, and z lengths of the iPhone measurements (x_i, y_i, z_i), as shown in equation (3) and (4). A scaling factor (C_n) is determined for the x, y, and z lengths, and can be applied to the model via a rescale function available on Meshlab. The values obtained for rescaling the models in this paper can be found in Table 12 of the 8. Appendix. Rescaling does not affect the number of vertices, since both the original and rescaled meshes contained the same number of vertices. This method could be better validated if the original model was available to make physical measurements between the landmarks. Instead, the validation is done virtually by the measurements of landmark distances given by Amsterdam UMC, and measured with the Vectra application, seen in Figure 33 (8. Appendix). The additional step of rescaling the mesh further slows down the mesh editing process, because it adds an additional step of manually obtaining lengths and determining the scaling factor, and could affect the final measurements if the rescale is done incorrectly. In the case of the Vectra and Eva scans, rescaling gives better results, since the magnitude of these scans are much larger than the physical model. However, if this is always required then this leaves another possible risk for human error, and further complicates quantitative 3D model analysis.

$$(3)\ scale\ factor\ for\ Vectra\colon (C_1, C_2, C_3) = \frac{(x_i, y_i, z_i)}{(x_V, y_V, z_V)}$$

$$(4)\ scale\ factor\ for\ Eva\colon (C_4, C_5, C_6) = \frac{(x_i, y_i, z_i)}{(x_E, y_E, z_E)}$$

The volumes of the breast phantom obtained from the iPhone, Vectra, and Eva scans show a general trend of overestimation, in contrast to the test objects. Some of the results are far out of range, with over 100% error, and therefore, cannot be trusted for clinical application. The larger the volume is, the larger the deviation of the 3D scans. The error percent ranges from 10%-114% for the iPhone, 15.3%-189% for the Vectra, and 32%-104% for the Eva. Some of these errors can also be attributed to torso reconstruction methods. The breast was segmented, and the torso was reconstructed as a flat geometry instead of curved, which increases the measured volume. However, comparing the differences by subtracting the base mesh avoids that issue, and the large errors remain. The large errors could be attributed to the watertight construction algorithm, which possibly adds additional volume around the mesh to fill any gaps. Unfortunately, this is not obvious to the naked eye, and volume cannot be obtained without making the mesh watertight. However, this error is minimal compared to the other factors that contribute to the large error, since the watertight mesh seems to be constructed tightly around the original mesh. Another factor that may attribute to the added volume is if the prosthetics are not attached seamlessly to the mannequin. The scanner may detect the seams, and the gaps in the seams can increase the volume. This would also explain why larger errors are seen for the larger prosthesis, whereas the smallest prosthesis of 75 cc had relatively smaller errors ranging from 10%-76%. The result of the scanner adding volume to the detected gaps can also explain why some of the measurements between the 100 cc and 125 cc models are not consistently increasing. In one case, the 125 cc model is detected as being smaller than the 100 cc model. In general, according to the large errors produced using these methods, it appears that the results cannot be trusted. However, the overall data shows that the smallest percent error from the iPhone measurement is 10%. Errors ranging from 10%-30% are not uncommon in previous studies that utilized low cost scanners [5]. However, for clinical use, this error is still higher than errors found in previous studies, which were at 1%-3% [23] and 2%-5% [1].

Type of issue	How significantly this contributed to error
Torso reconstruction method is flat instead of curved	Large, significant: Does not accurately represent the true breast shape and true measurements.
Bound definition for breast segmentation	Large, significant: Bounds influence the shape of the breast and measured volume.
Watertight construction algorithm	Small, minimal: Watertight mesh is constructed tightly to the original mesh
Scanner detects seams and gaps from prosthesis	Medium: Explains why larger models resulted in larger error while the smaller models did not, and

	the inconsistent increase of volumes between the 75 cc and the 100 cc/125 cc models

Table 9: Summary of the issues encountered with processing the meshes, and how significantly these issues influenced the volume results

5.1.5 Clinical workflow

As for the overall workflow for using 3D scans in a clinical setting, it can be concluded that there are some steps that remain the same across any scans, regardless of the geometric details. The overall clinical workflow is illustrated in Figure 29. The main steps consist of acquiring the mesh, preprocessing the mesh for measurements, analyzing the mesh, and exporting the mesh or the resulting measurements. The specific functions within each step are laid out and necessary for any 3D scan obtained, regardless of the tool used. In most cases until 3D scans further improve, at least one of these functionalities is a necessary step in this process. Furthermore, cleaning the mesh, closing holes, and making the mesh watertight is a manual process, and unique to the anatomy or shape being inspected. While this is not an automated function, the analysis step has been automated with the improvement of software. If the mesh is clean and watertight, the software can easily calculate volume/area, which is very useful for complex shapes. The final step is exporting the mesh, whether as a 3D visualization for a digital model or to a 3D printer for a physical model; the accompanying data should be transferrable.

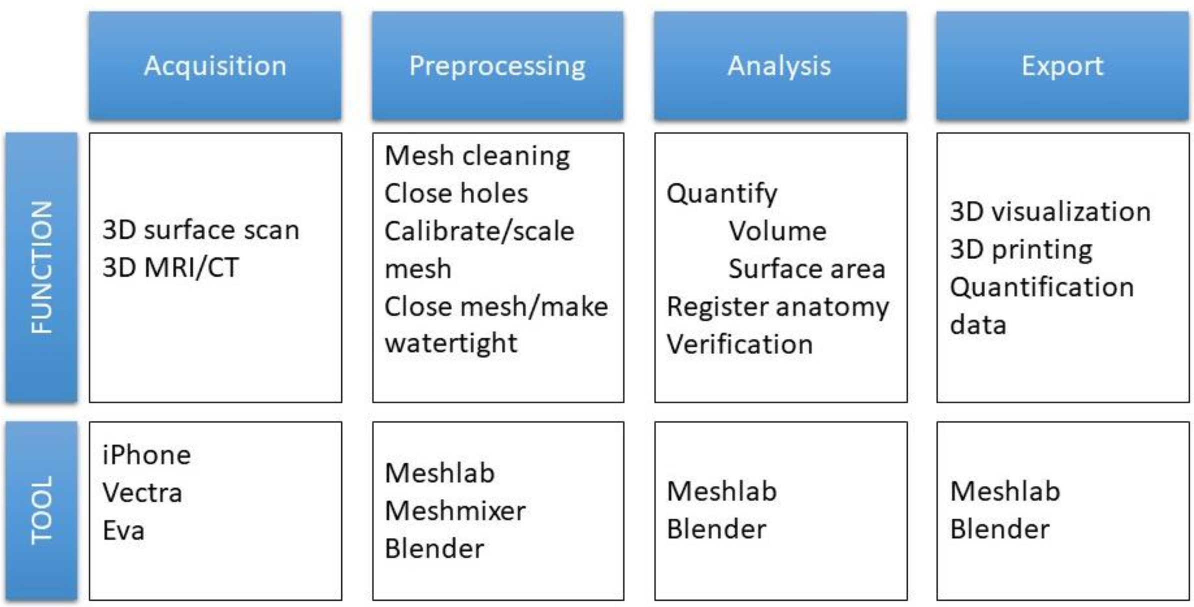

Figure 29: Clinical workflow for 3D scanning and quantification

Based on the experience acquired throughout this study, Meshlab and Meshmixer are the recommended software to use for a new to experienced user. Meshmixer is versatile in making any shape watertight, while Meshlab can perform all the functions from mesh cleaning during preprocessing to quantifications during analysis. Although Blender is also capable of this, the software's ability to handle multitude of functions, ranging from modeling to video animation, may be overwhelming for new users to learn. Training a new user on specific tasks in Meshlab and Meshmixer is quick if the steps are predefined and the segmentation is simple. The preprocessing step requires the most focus for consistency among different models, and will vary with user experience. However, in this study, given predefined steps for preprocessing, the whole process to export took 5-10 minutes for a 3D visualization with quantifications. If this process resulted in accurate measurements, it would be beneficial for select patients in clinics.

5.2 Limitations

The first limitation of using the iPhone X for 3D scanning is how the front facing camera makes keeping the object of interest within frame difficult. The half globe and styrofoam objects were scanned manually, and required space to walk smoothly around the object while maintaining a steady hand. This needed to be done multiple times before obtaining a usable scan. An option to overcome this difficulty is to attach a second iPhone to the first iPhone to act as a display. Similarly, screen mirroring to a PC or TV using other free or paid applications are available. The breast phantom measurements were taken with the iPhone, fixed to a tripod with a moving arm; this appeared to make scanning easier, however, it was not possible to obtain a full 360˚ scan. Although this study did not require a full 360˚ scan, this can be a limitation for other applications. A 360˚ scan of the torso could help validate the torso circumference, since this is relatively simple to measure physically. Placing the object on a rotating turntable to scan would not produce a successful 3D scan, because the object cannot be moved to produce a complete mesh. This is likely because the software requires consistent lighting and background information in order to create the 3D scene.

A second limitation of using the iPhone in conjunction with software is the diverse nature of reconstructing a watertight model. This is straight forward for simple geometry, such as a hemisphere. However, this type of geometry is rarely found in human anatomy, so some improvisation, manual techniques, and knowledge of 3D geometry is involved. Developers could address this by also including machine learning techniques, which could automatically reconstruct the breast torso for any breast model. In order for this to happen, the system will need a database of hundreds of examples in order to create a neural network. Therefore, it is possible to apply AI techniques to 3D modeling of specific anatomies.

5.3 Recommendations & future research

Considering how similar the results from the iPhone are to those from clinically approved devices, such as the Vectra and Eva, it is worth further exploring how to process iPhone scans for clinical use. To improve the acquisition of the iPhone scans from a front facing camera, fixing the iPhone to a track with the object in the center as shown in Figure 31, could ease the scanning procedure of small objects [3]. In clinical use, a scaled up version will be needed in order to scan a human torso. Finally, to improve the overall model when processing the mesh, more complex geometry modeling techniques, such as curved planes, should be used. However, it is important to properly identify the breast bounds. It would be helpful to also have access to a model with breast attributes, so there is better control as to how the bounds are defined. Various breast bound methods were discussed in this paper, and the most common points of interest were used in this study to define the breast boundaries. Using the iPhone scan along with an MRI scan to obtain the chest wall curvature would provide a more complicated mesh geometry, but more accurate results. Since this method is more costly and not practical, another method for recreating the chest wall is by using a computational method called Coons patch. This method is able to recreate a curved surface given landmark points, such as the breast bounds along the IMF.

Figure 30: iPhone X 3D scanning track [3]

6. Conclusion

This study aimed to explore the iPhone 3D scanning functionalities, how it compares to established 3D scanners currently used in clinics, and possible application in a clinical environment. In order to segment the breast model, various breast boundaries that were used in different research papers were presented. Folding line method seems to be the most commonly used when outlining the upper curve of the breast, while the bottom curve is generally defined by using points along the IMF. However, most of the variation comes from the method of recreation of the chest wall, which is largely influenced by the breast landmarks. Within this study, the landmarks provided by the Vectra system were used for segmenting the breast model. To determine the necessary steps to process a 3D mesh and the metric measurements, a simple hemispherical object was used. These results allow us to understand the magnitude of the exported data and identify what segmentation processes are required, when this is applied to a complex model of a human torso. Mesh processing applications, such as Meshlab, Meshmixer, and Blender, all contained helpful tools for segmenting and sealing the 3D mesh for volume measurements. The obtained volumes of the hemisphere objects compared these different processing applications, all of which resulted within 10% error of each other. Some of the underestimated error could be explained by the preprocessing of the mesh and removing some of the data before closing the mesh. After the mesh process was validated, it was applied to the breast phantom models. In contrast to the hemisphere test objects, the segmentation was a lot more complex. Due to the difficulties in recreating the chest wall using the specified software, no useful clinical data could be acquired using any of the scanning methods. It is apparent, however, that this process could yield adequate results applied to symmetrical phantoms, such as the hemisphere. Therefore, these preprocessing methods need to be improved for breast scans, which will possibly provide more reasonable results with smaller error. The general clinical workflow for 3D scanning and quantification is mesh acquisition, mesh processing, analysis, and exportation. While the details in mesh processing vary depending on the geometry and quality of the scan, it is a crucial and required step for all 3D scans.

7. References

1. O'Connell, R.L., et al., *Validation of the Vectra XT three-dimensional imaging system for measuring breast volume and symmetry following oncological reconstruction.* Breast Cancer Res Treat, 2018. **171**(2): p. 391-398.
2. Kovacs, L., et al., *Comparison between breast volume measurement using 3D surface imaging and classical techniques.* Breast, 2007. **16**(2): p. 137-45.
3. Thingiverse, M. *iPhone X, XR, XS, XS Max, 11, 11 Pro/Max rotating 3D scanner*. 2020; Available from: https://www.thingiverse.com/thing:3438302.
4. Verdaasdonk, R., et al., *The iPhone X as 3D scanner for quantitative imaging of body parts for diagnosis and treatment follow-up.*
5. Choppin, S.B., et al., *Breast Volume Calculation Using a Low-Cost Scanning System*, in *Proceedings of the 4th International Conference on 3D Body Scanning Technologies, Long Beach CA, USA, 19-20 November 2013*. 2013. p. 12-20.
6. Bulstrode, N., E. Bellamy, and S. Shrotria, *Breast volume assessment: comparing five different techniques.* Breast, 2001. **10**(2): p. 117-23.
7. Mikolajczyk, M., A. Kasielska-Trojan, and B. Antoszewski, *A New Tool for Breast Anthropometric Measurements: Presentation and Validation for Women and Men.* Aesthetic Plast Surg, 2019. **43**(5): p. 1160-1170.
8. Lee, H.Y., K. Hong, and E.A. Kim, *Measurement protocol of women's nude breasts using a 3D scanning technique.* Appl Ergon, 2004. **35**(4): p. 353-9.
9. Lee, W.Y., et al., *Three-Dimensional Surface Imaging is an Effective Tool for Measuring Breast Volume: A Validation Study.* Arch Plast Surg, 2016. **43**(5): p. 430-7.
10. Treleaven, P. and J. Wells, *3D Body Scanning and Healthcare Applications.* Computer, 2007. **40**(7): p. 28-34.
11. Daniell, N., T. Olds, and G. Tomkinson, *Volumetric differences in body shape among adults with differing body mass index values: An analysis using three-dimensional body scans.* Am J Hum Biol, 2014. **26**(2): p. 156-63.
12. Haleem, A. and M. Javaid, *3D scanning applications in medical field: A literature-based review.* Clinical Epidemiology and Global Health, 2019. **7**(2): p. 199-210.
13. Zancanaro, C., et al., *Reliability of Three-dimensional Photonic Scanner Anthropometry Performed by Skilled and Naïve Operators.* International Journal of Ergonomics (IJEG), 2015. **5**(1).
14. Tokkari, N.V., Rudolf M.; Liberton, Niels, *Comparison and use of 3D scanners to improve the quantification of medical images (surface structures and volumes) during follow up of clinical (surgical) procedures*. VU University Medical Center. p. 10.
15. Pears, N., Y. Liu, ;, and P. Bunting, *3D Imaging, Analysis, and Applications.* Springer, 2012: p. 506.
16. Tzou, C.H., et al., *Comparison of three-dimensional surface-imaging systems.* J Plast Reconstr Aesthet Surg, 2014. **67**(4): p. 489-97.
17. Verhulst, A., et al., *Three-Dimensional Imaging of the Face: A Comparison Between Three Different Imaging Modalities.* Aesthet Surg J, 2018. **38**(6): p. 579-585.
18. Europe, A. *Artec 3D scanners*. 2020 8 June 2020]; Available from: https://www.artec3d.com/.
19. Cardinal, D. *How Apple's iPhone X TrueDepth Camera Works*. 2017; Available from: https://www.extremetech.com/mobile/255771-apple-iphone-x-truedepth-camera-works.

20. Cignoni, P., et al., *Meshlab: an Open-Source Mesh Processing Tool*. Eurographics Italian Chapter Conference. Vol. 2020. 2008: The Eurographics Association.
21. Inspect, G.; Available from: https://www.gom-inspect.com/en/overview.php.
22. Roosendaal, T. *Blender*. [cited 2020; Available from: www.blender.org.
23. Kovacs, L., et al., *New aspects of breast volume measurement using 3-dimensional surface imaging.* Ann Plast Surg, 2006. **57**(6): p. 602-10.

8. Appendix

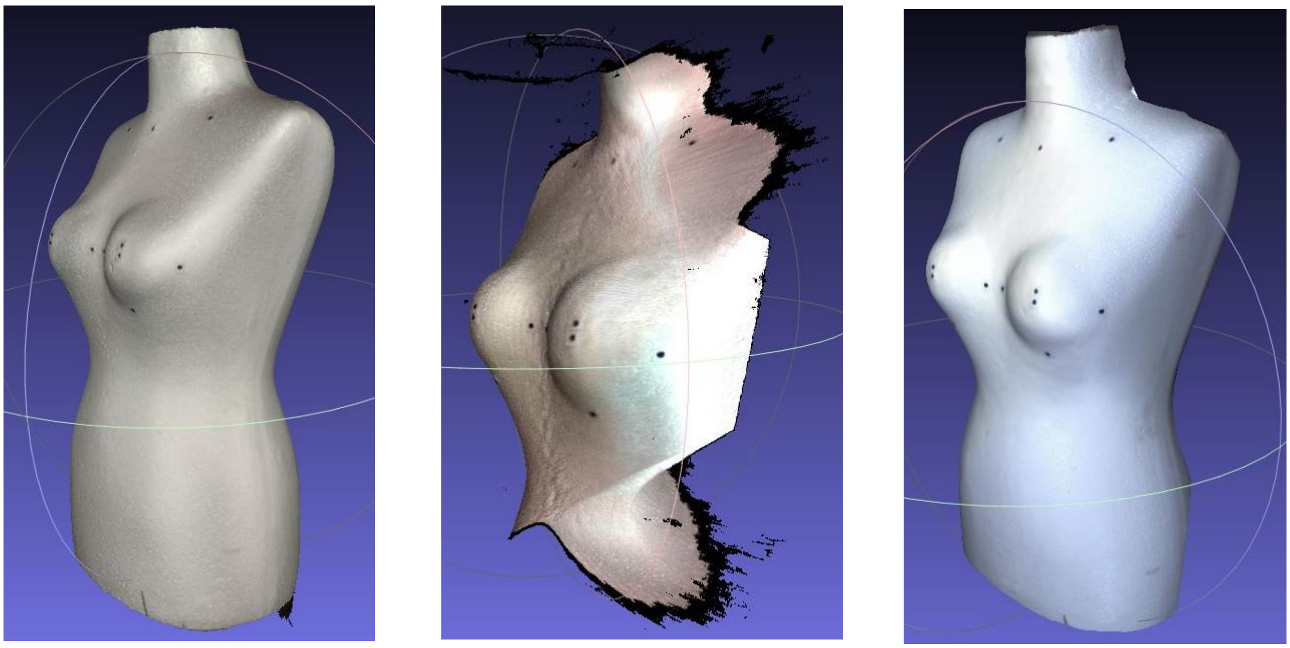

Figure 31: From left to right, scans of the 0 cc torso taken using an Eva, iPhone, and Vectra

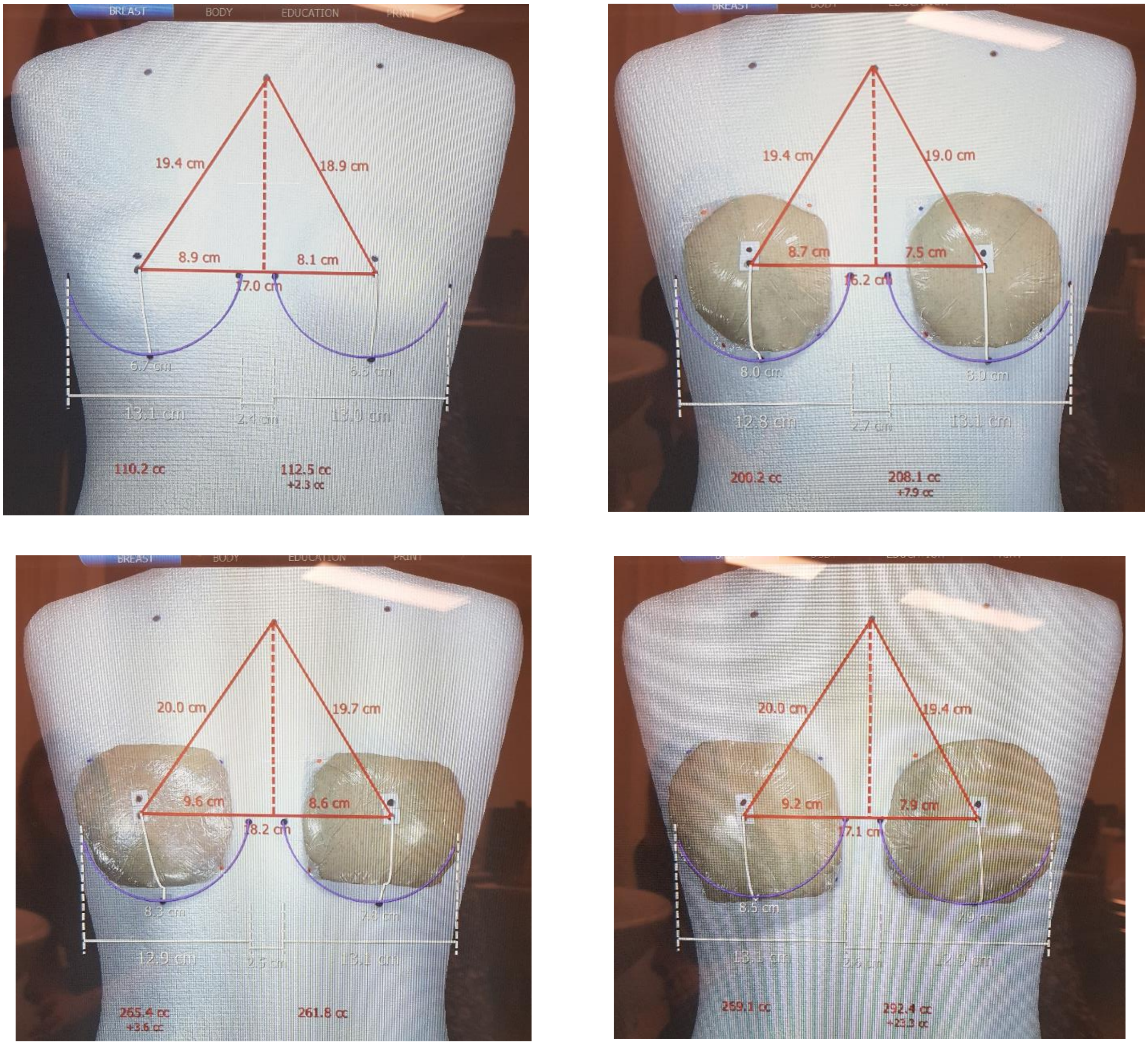

Figure 32: Length and volume measurements provided by Vectra breast measurement application

	Half globe	Volume	Area	Styrofoam	Volume	Area
Measured base circumference (cm)						
1	48.1	939.62	552	19.7	64.55	92.6
2	48	933.76	550	19.6	63.58	91.8
3	48.1	939.62	552	19.7	64.55	92.6
4	48.1	939.62	552	19.6	63.58	91.8
5	48	933.76	550	19.6	63.58	91.8
6	48	933.76	550	19.7	64.55	92.6
7	48.1	939.62	552	19.6	63.58	91.8

8	48.1	939.62	552	19.6	63.58	91.8
9	48.1	939.62	552	19.6	63.58	91.8
10	48	933.76	550	19.6	63.58	91.8
Mean	48.1	**937.3**	**551**	19.6	**63.87**	**92.04**
SD	0.049	2.871	0.980	0.046	0.44451	0.367
V(C) using mean (cc)	939.62			63.58		
A(C) using mean (cm2)	552.33			91.71		
Measured diameter (cm)						
1	15.1	901.4	537.2	6.2	62.4	90.6
2	15.2	919.4	544.4	6.23	63.3	91.5
3	15.2	919.4	544.4	6.1	59.4	87.7
4	15.2	919.4	544.4	6.18	61.8	90
5	15.3	937.7	551.6	6.2	62.4	90.6
6	15.2	919.4	544.4	6.23	63.3	91.5
7	15.2	919.4	544.4	6.2	62.4	90.6
8	15.2	919.4	544.4	6.23	63.3	91.5
9	15.2	919.4	544.4	6.23	63.3	91.5
10	15.2	919.4	544.4	6.23	63.3	91.5
Mean	15.2	**919.43**	**544.4**	6.203	**62.49**	**90.7**
SD	0.04	8.1171	3.21994	0.038484	1.154513	1.12783
V(r) using mean (cc)	919.4			62.48		
A(r) using mean (cm2)	544.4			90.66		

Table 10: Radii, volume, and area calculations for the half globe and styrofoam objects with calculated average and standard deviations. Volume/Area was calculated using average of the diameter/circumference and average individual volume/area calculations (red). Both give similar results when rounded to 3 significant figures.

		Faces	Vertices
iPhone	base (0 cc)	1057680	539,650
	75 cc	1122673	570662
	100 cc	1116515	566871
	125 cc	1114200	566329
Vectra	base (0 cc)	63141	31622
	75 cc	59973	30039
	100 cc	61149	30620
	125 cc	60360	30230
Eva	base (0 cc)	500000	251355
	75 cc	500000	253009
	100 cc	499999	255135
	125 cc	500000	255794

Table 11: Number of faces and vertices for the breast phantom meshes, scanned by the iPhone, Vectra, and Eva. Count was taken before segmenting and after cleaning. Surface areas differ.

	x	y	z
iPhone	0.0762	0.1706	0.2253
Vectra	71.4314	170.0766	229.1795
Eva	69.9338	170.6356	231.3164

Vectra	C1	0.0011
	C2	0.0010
	C3	0.0010
Eva	C4	0.0011
	C5	0.0010
	C6	0.0010

Table 12: Length measurements in x, y, and z direction for breast model scanned by iPhone, Vectra, and Eva. These measurements are used to determine the scaling factors shown in the right table.